Addis Ababa University

College of Technology and Built Environment(CTBE)

School of Electrical and Computer Engineering

Model Predictive Speed and Torque Control of Induction Motor for Electric Vehicle

A thesis submitted to School of Graduate Studies, College of Technology and Built Environment, Addis Ababa University in partial fulfillment of the requirement for the Degree of Master of Science in Electrical Engineering (Control Engineering).

By

Tsion Nigusse

Advisor

Dr.Mengesha Mamo(PHD)

July,2025

Addis Ababa, Ethiopia

Addis Ababa University

College of Technology and Built Environment(CTBE)

School of Electrical and Computer Engineering

Model Predictive Speed and Torque Control of Induction Motor for Electric Vehicle

By:**Tsion Nigusse**

APPROVED BY BOARD OF EXAMINERS

Name	Signature	Date
_____	_____	_____
(Dean, School of Graduate Committee)		
_____	_____	_____
(Advisor)		
_____	_____	_____
(Internal Examiner)		
_____	_____	_____
(External Examiner)		

Declaration

I declared that this MSc thesis is my original work and has not been presented for any degree in university or college, and sources of materials used for the thesis is well acknowledged.

Name Signature

_____ _____

Place:

College of Technology and Built Environment,CTBE

Addis Ababa University,AAU

Addis Ababa,

Ethiopia.

Submitted in:July,2025

This thesis has been submitted for examination with my approval as a university advisor.

Advisor **Signature**

_____ _____

Acknowledgment

I want to express my gratitude to my adviser, Dr. Mengesha Mamo, for his invaluable support and the insightful information he provided me during the entire project. I have learned a lot from his thoughts, insight, and prudence. Additionally, I want to thank Dr. Dereje Shiferaw and Dr. Lebsewerk Negash for their time spent analyzing and monitoring my work as well as for their insightful recommendations. Finally, I want to thank my friends, family, and coworkers for their support and for helping me to overcome numerous challenges during my research journey.

Abstract

This thesis proposes, a model predictive controller in order to control the speed and torque of the induction motor. The induction motor has several interesting benefits, including simplicity, affordability, robustness, high efficiency, and flexibility features makes it a desirable choice for electric vehicles (EV) applications.

A cascaded control structure is used, which has an external loop and an internal loop. Where the external loop is used for controlling the speed of the motor, and result were verified through MPC,ISMC and LQR controllers. The inner control loop is based on Finite Control Set Model Predictive Torque Control (FCS-MPTC), which allows precise torque control, fast dynamic response, and ease of implementation. It uses the output of speed controller as a reference and the mathematical model of the motor for estimation, prediction, and optimization. In addition, discretizations were made using the forward euler approximation on a given sampling period. In addition, to achieve good dynamic performance, the motor is powered by 2L-VSI. These models were integrated and simulations were carried out using Matlab/Simulink.

As shown in the results, both MPC and ISMC have good disturbance rejection capability. However, LQR has a larger steady-state error in the presence of sudden disturbance.

Keywords: Induction Motor, EVs, MPC, LQR, FCS-MPTC, 2L-VSI , ISMC

Contents

List of Figures

List of Tables

Nomenclature

FCS-MPTC Finite Control Set Model Predictive Torque Control

2L-VSI Two Level Voltage Source Inverter

AC Alternating Current

BLDC brush-less DC motor

DTC Direct Torque Control

EMF) Electromotive Force

Ev Electric Vehicle

FOC Field Oriented Control

IM Induction Motor

ISMC Integral Sliding Mode Control

LQR Linear Quadratic Regulator

MPC Model Predictive Controller

NLP Non-linear Programming Problem

OCP Optimal Control Problem

PFC Predictive Flux Control

PMSM permanent magnet synchronous motors

PTC Predictive Torque Controller

Chapter 1

Introduction

In this chapter, background of the study, statement of the problem, objectivity, scope, methodology, and thesis outline are discussed.

1.1 Background of Study

Currently, countries are attempting to minimize CO_2 emissions significantly. Since internal combustion engines power most automobiles, they are among the most significant sources of these pollutants. On basis of several researches, cars and trucks are responsible for almost 25% of CO_2 emissions [28]. The usage of internal combustion engine vehicles results in higher carbon emissions; however, electric vehicles (EVs) are playing a crucial role in lowering air pollution because they use electric motors for propulsion. It consists of sub components such as an electric motor, controllers, converter, battery, and mechanical transmission[37].

Choosing the appropriate type of electric motor is one of the crucial decisions that must be made in the construction of an electric vehicle. Features like easy controllability, good efficiency, cost effectiveness, and simple designs has to be considered [8]. Such as, DC motors, brush-less DC motors (BLDC), induction motors (IM), permanent magnet synchronous motors (PMSM), and switching reluctance motors (SRM), are some of electric motors used in electric vehicles.

Because they are easy to regulate and have a linear speed-torque characteristic, DC motors are chosen. However, they cannot be widely used on medium- and large-sized EVs due to commutator and brush architectures as well as maintenance issues. However, advances in magnet technology have made it possible to raise efficiency of PMSM. However, there are still drawbacks to permanent magnet motors, such as the expensive cost of magnetic materials and the possibility of demagnetization. An additional option SRMs are widely used due to their affordability and ease of production; nevertheless, due to their noise and large torque ripple, they are not suitable for higher-speed applications[37].

This thesis utilizes an induction motor for a numerous of reasons. [16, 3]. They are inexpensive in manufacturing and services. Moreover, they are extremely robust under different operational and environmental conditions. Poor speed regulation and non-linear mechanical characteristic, are some of the classical drawbacks of IMs. These days A number of control techniques have been proposed to control IM due to the emerging technology of power electronics and microprocessor. Several control schemes have been suggested to control IM, Sector control schemes are common today in control-of speed, torque, and flux of induction motor. FOC (field-oriented control) and DTC (direct torque control) are most commonly used ones. Since its introduction in the late 1970s, the FOC algorithm has found widespread usage in industry. Because it has good steady state and fast dynamic response[34]. But the torque generating current I_q and flux current I_d must be controlled separately which makes control system complex.

In the variable speed drive applications, direct torque control (DTC) is a high performance control algorithm[39]. It offers fast dynamic response with simple structure. The proper voltage vector is chosen directly from a precomputed switching table on the basis of the stator flux vector position and signs of the torque and flux errors. The main disadvantages of DTC are large torque and flux ripples. It chooses the optimum voltage vector from a pre-defined switching table, that is not always the best one, particularly in the low speed range[40].

Model predictive control (MPC) has emerged as a great topic of interest in power electronic and motor drives due to its simple design, fast-response while handling constraints[38]. The first proposal on MPC is found in [17], where MPC is combined with classical PWM strategy. In recent papers on MPC to hinder PWM it applies the optimal voltage vector directly to the inverter [27].

Model Predictive Torque Control(MPTC), is the terminology used when MPC is applied in motor drives with the objective of torque control, and which has been suggested as an effective alternative to conventional DTC. MPTC employs online optimization to substitute the conventional switching table. A cost function which is the torque error and the flux error is established and chooses the best voltage vector in trying to minimize the cost function. Therefore, MPTC employs more precise and efficient voltage vector than conventional DTC[15]. In this paper MPC controller used to control speed, torque and flux of the the motor which are used for electric vehicle application.

1.2 Problem Statement

Twenty-five percent of the world's fuel requirement originates from the energy consumption of transport and is bound to expand exponentially with an adverse impact on nature in the context of climate change [33]. Thus, in this paper induction motor has been employed for electric vehicle application. Induction motor (IM) drives are utilized in any type of steady-state and dynamic applications. They are popular in the the recent world industries because of their high efficiency and durability. IMs are cheap in production and services, and they are very durable under a wide range of operating and environmental conditions.

Some Induction motor uses classical control system to control the speed and motor torque, which is a complicated system since it has three or more controllers for a specified system. Compared to Model Predictive Control (MPC) strategies, longer settling time and high overshoot are not favorable for this control strategy. Therefore, in this paper, MPC is designed to minimize the complexity and maximize dynamic performance of the controller.

1.3 Objectives

1.3.1 General Objective

The general objective this thesis is designing and simulating of model predictive speed and torque control of induction motor for an electric vehicle.

1.3.2 Specific Objective

- To model and simulate an induction motor with electric vehicle as a load.
- To design MPC, ISMC, and LQR controllers and implement to the system.

- To test the performance using simulation.

1.4 Methodology

Procedure	Specific tasks
Literature review	Doing research on published research papers, books, and articles related to this topic.
Modeling of a induction motor	Develop state space model of induction motor based on its dynamics.
Model verification	Verify the modeled induction motor using Simulink
Modeling of EV load	Mathematical modeling tractive force load for ev application to use as a disturbance for induction motor
Using on the obtained model	Design MPC, ISMC, and LQR for reference stabilization.
Simulation	To examine the controller and whole system.

Table 1.1: Over all thesis procedure

1.5 Scope and Significance of the Research

Model Predictive control of induction motor is less susceptible to system uncertainty due to which the future action of the plant is also taken into consideration in the controller design; and at each step an optimization is conducted online so that the future anticipated plant follows the required reference.

There are certain control techniques in literature that are used to regulate speed and torque of induction motor but, in this work mpc is programmed in MATLAB/SIMULINK to derive good dynamic response and low current ripple during the existence of disturbance and parameter changes. To accomplish the aforementioned general and specific objectives, the research effort is limited to model predictive control (MPC) design for speed and torque control of induction motor.

1.6 Thesis outline

Chapter 1 deals with an introduction to the system and offers insight into the issues that will be discussed later. It essentially gives an overview of the entire system.

In chapter two various literatures are explained and analyzed. In this chapter operation principles, torque generation, and the theoretical background of IM are clarified. In addition, the proposed controller theory, two-level voltage source inverter, and other associated studies are explained in this chapter.

In chapter three, induction motor modeling and verification were carried out in MATLAB/SIMULINK and also tractive force modeling for electric vehicle at rated speed and load curve design undertaken in MATLAB/SIMULINK.

The overall controller design techniques are considered in chapter four.

And chapter five deals on the simulation results and discussion.

The conclusion and suggestions for future work are presented in Chapter six.

The list of references used in this thesis is arranged numerically. The appendix contains additional ideas and proofs that are pertinent to this work.

Chapter 2

Literature review

This chapter covers generation of torque, operation principles, and the unique characteristics of IM. Also, the theory of the proposed controller, two-level voltage source inverter, and other related works are included in this chapter.

2.1 Induction Motor

Asynchronous or induction motors are one type of electric motor that is frequently used to power electric vehicles (EVs). Through electromagnetically inducing current from the stator winding's magnetic field, it produces torque in the rotor. Therefore, it uses electromagnetic induction to transform electrical energy into mechanical energy with no physical connection to the rotor. Because of their great flexibility, efficiency, and relatively simple design, induction motors can be used for several electrical applications[25].

The operation of induction motors is based on the electromagnetic induction concept. When the stator winding of a motor is energized by an AC power source, a rotating magnetic field results. A magnetic field in the rotor is built up due to the revolving magnetic field inducing currents in the rotor winding by electromagnetic induction. As a result of the interaction between the revolving magnetic fields of the stator and the rotor, torque is produced that drives the motor and vehicle[11].

Asynchronous motors do not require a physical connection between the rotor and the stator, in contrast to synchronous motors that rely on permanent magnets. Rather, the rotating magnetic field that powers the rotor in asynchronous motors is produced via electromagnetic induction.

A three-phase induction motor in an electric car has three windings in the stator that

are electrically separated from each other by 120 degrees. This enables the motor to rotate continuously and effortlessly without any extra components, like a gearbox, to power the wheels from the battery.

Both squirrel cage rotor and wound rotor induction motor are used EVs applications. Squirrel cage rotors are the most commonly used induction motor, due to their simple construction, high reliability, and very low maintenance requirements. But in case of wound rotor have a complex construction with externally accessible rotor windings, which require more maintenance. In this thesis, squirrel cage induction motor is used for EV applications.

2.1.1 Working Principle of Induction Motor

The relationship between a rotating magnetic field and the current induced in the rotor windings is how the three-phase squirrel cage induction motor works. Here is a thorough explanation:

- The three-phase induction motor's stator windings produced a rotating magnetic field when they are connected to an AC power source; the synchronous speed (NS) of this magnetic field is based on the supply frequency (f) and the number of poles (p) in the stator winding.

- The rotating component of an induction motor is called the rotor, and it is usually constructed as a "squirrel-cage" with conducting bars inserted in a metallic core. The rotating magnetic field produced by the stator windings induces a voltage (electromotive force or EMF) in the rotor bars, in accordance with Faraday's law of electromagnetic induction.

- The induced voltage in the rotor bars creates a current flow in the rotor circuit, in accordance with Ohm's law. The interaction between the rotor current and the stator's rotating magnetic field creates a force on the rotor bars, which results in a torque that causes the rotor to start rotating. The synchronous speed (Ns) of the stator's rotating magnetic field is always greater than rotor's rotational speed (Nr).

- Slip refers to the variation between the synchronous speed (Ns) and the rotor speed (Nr). which is typically expressed as a percentage and calculated as: $s = (Ns - Nr)/Ns$. It determines the produced torque the speed of the induction motor.

- **I**nduction motors can produce a starting torque to overcome the initial load, which is important for starting the motor. As the motor reaches its running speed, the torque produced is sufficient to maintain the desired load. The starting torque and running torque of an induction motor are affected by factors such as the rotor design, supply

voltage, and load characteristics.

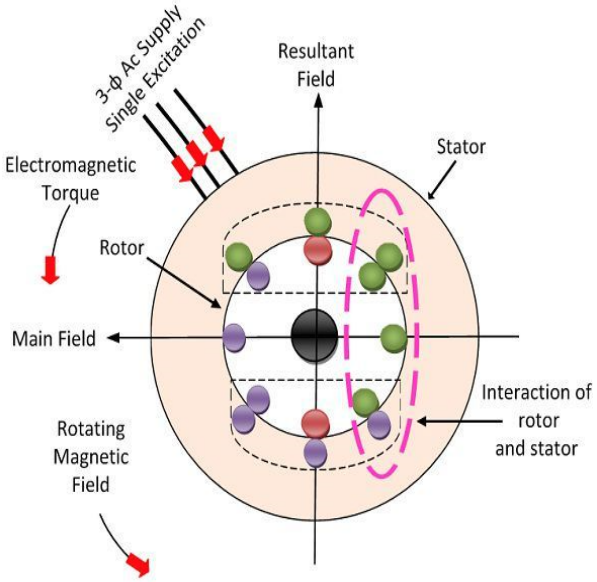

Figure 2.1: Working principle of 3-phase induction motor

2.1.2 Advantage of Induction Motor

- **Robust and Reliability**: induction motors are robust in construction and to withstand harsh operating conditions, making them highly reliable and durable in EV applications.
- **High torque at low speed**: has the ability to provide high torque at low speeds, which is important for EVs during startup and for hill climbing. This torque capability is made possible by the design of the rotor and stator, also power electronics used to control the performance of the motor.
- **Cost-effectiveness**: They can be more affordable than other motor types, like permanent magnet motors, because they don't require permanent magnets on the rotor construction.
- **Low drag when rolling**: When an electric vehicle (EV) is moving with no power, the electric motor will have a drag effect. It is due to electromagnetic forces in the motor, which can counteract the movement of the rotor and create resistance against moving the motor. Since, there is no permanent magnet in the rotor of induction motor the drag is usually less than in permanent magnet motors. This is because induction motors use electromagnetic induction to create the rotating magnetic field

in the rotor, which induces current and generates magnetic forces which resist rotor movement. Therefore, when an induction motor is not driven, the vehicle will roll with less friction and the motor drag is often lower.

2.2 Two Level Voltage Source Inverter

Two-level voltage source inverter (VSI) is a kind of power electronics which used to convert direct current (DC) into alternating current (AC). Due to its wide availability, high dynamic performance, and simplicity, this converter topology is frequently used in drive applications. As seen in 2.2. the converter supplies power to an induction machine in a typical drive application. As illustrated in 2.3. this topology can generate eight distinct voltage vectors due to the characteristics of the converter. Two zero vectors (v0 and v7) and six active voltage vectors can be distinguished[14]. The switching converter's states determine the voltage vectors as follows:

$$S = \frac{2}{3}(S_a + e^{j2\pi/3}.S_b + e^{j4\pi/3}.S_c) \tag{2.1}$$

where S_a, S_b, S_c stand for each leg's switching state, as shown in the 2.2. The output voltage vector can be expressed as follows[14],

$$Vs = vdc.S \tag{2.2}$$

where, v_{dc} is dc voltage source to the inverter

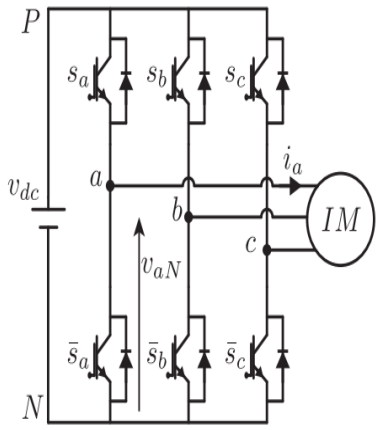

Figure 2.2: 2L-VSI.

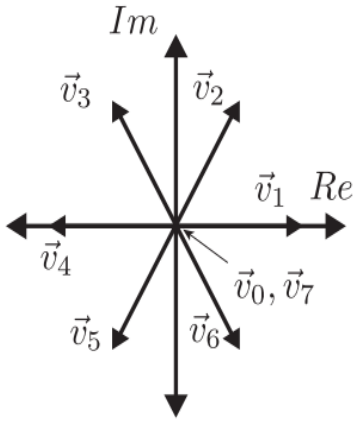

Figure 2.3: Voltage vectors of 2L-VSI.

2.3 Model Predictive Controller

Model Predictive Control (MPC) is a modern control technique that solves a finite-horizon optimization problem at each time step to maximize control inputs to a system. The following are some of the main characteristics and ideas of MPC[12]:

- **Prediction Model**: MPC forecasts future behavior over a specified horizon using a model of the system. This model may be non-linear or linear.
- **Optimization**: MPC solves an optimization problem at each time step in order to minimize a predetermined cost function, which contains terms for error tracking and control effort.
- **Constraints Handling**: MPC can explicitly incorporate constraints on inputs, states, and outputs, which makes it suitable for systems with physical limitations.
- **Receding Horizon**: As time progresses, MPC continuously updates its predictions and optimization, which is known as receding horizon.

The fundamental process for designing an MPC controller is outlined in Paper [21]. Creating a mathematical model of the system dynamics is the first step. Secondly, establish a cost function that measures performance, like error tracking. Next, formulate the optimization problem while taking the cost function and constraints into account. Applying the first control input and repeating the process in the subsequent time step is the last step after resolving the optimization problem to determine the best control inputs for the current time step.

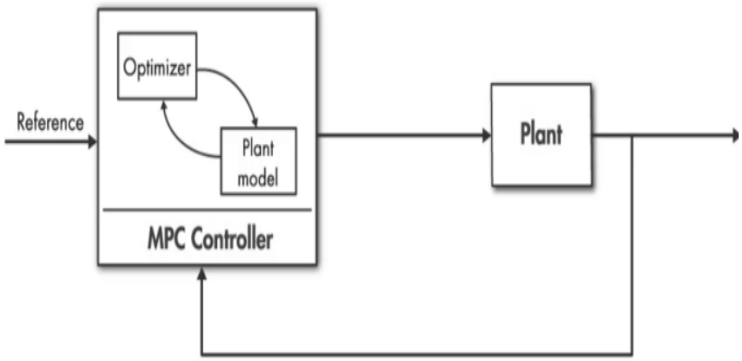

Figure 2.4: Block-Diagram of MPC based control loop

2.4 Related Works

In [19] model predictive torque control of an induction motor is stated for the application of electric vehicles and the result is verified for small load torque(10Nm) but in this paper the higher load torque is considered for model verification upto 150Nm. In [10] direct torque control of induction motor is implemented but in this paper model predictive torque control is used which reduce the torque ripple, energy loss associated with the DTC.

In [9] uses LQR controller for controlling the speed of induction motor which optimizes across the entire time window (horizon) where as MPC optimizes in a receding time window which has advantage on variable speed application such as for electric vehicle. Also, when load torque is applied on the speed controller as disturbance the result has higher steady state error in this paper non-liner model predictive controller is used in order to have good controller performance.

In [23] implemented cascaded control system which is predictive torque control technique used for controlling torque and flux of the motor but PI controller is used for controlling the speed of induction motor which has some drawbacks, such as: complicated control structure, limited robustness to the parameter changes, and limited control performance. But in this project MPC based controller is used in order to compensate the above drawbacks.

In [14] implemented cascaded control system which is predictive current control technique used for controlling current of the motor but in this thesis predictive torque control for having good performance in torque result.

paper [7] stated on integral sliding mode speed control of induction motor which is robustness and reduce chattering during the steady state. Parameter tuning is crucial part in this controller for having better performance. In this thesis ISMC speed control of induction motor were conducted and its performance were verified in matlab/simulink and compared to mpc controller.

Paper [21] states different types of model predictive control (MPC) for induction motor. The most common control technique of induction motor are Field Oriented Control(FOC) and Direct Torque Control(DTC) but in modern induction motor drive needs additional requirements for control performance due to higher degree of digitalization, more precise control objectives and faster system speed response. MPC research high demand in the field of motor drive due to its simple principle and convenient implementation. There are different MPC control technique for induction motor such as:

- **Predictive Current Control(PCC)**: Its control method is comparable to that of

FOC; stator currents are chosen as control parameters and utilized for cost function optimization and necessary prediction.

- **Predictive Torque Control(PTC)**: It has similar control technique as FOC. It uses torque and flux as control parameter and these are used for required estimation, prediction and cost function optimization.
- **Predictive Flux Control(PFC)**: it is the same as PTC but In order to remove the weighting factor from the cost function, stator flux control is used in place of the torque and flux-based cost function.

In this paper predictive torque control is used due to its advantages of no field orientation, simple structure, and rapid response.

2.5 Electric Motors for EV Application

Currently, due to the fact that internal combustion engine vehicles increase carbon emissions, and countries remain dependent on oil-importing countries. In order to provide a number of exceptional features, including wide-torque speed range, high efficiency, lower maintenance costs, and less air pollution, EVs use electric motors rather than internal combustion engines.

Using the electrical energy stored in the battery, an electric motor propels the EV forward. The battery, electric motor, power controller, and mechanical transmission are some of its sub-components. When it comes to EV applications, the electric motor selection is extremely important. When choosing a motor, factors like high power density, straightforward design, low maintenance costs, and easy controllability must be taken into account. Electric motors of various types, including DC motors, brushless DC motors (BLDC), induction motors (IM), permanent magnet synchronous motors (PMSM), and switched reluctance motors (SRM), are used in electric vehicle applications.

Due to the need for high torque at low speeds, DC motors were initially employed in EV applications. However, friction between the brush and collector, which transfers the armature current, prevented them from meeting the necessary amount at higher speeds. Furthermore, it requires maintenance for the brush-collector arrangement and is less efficient than other motor types[6]. The other one is BLDC motor which operates on direct current. unlike DC motor it uses electronic commutation to switch the direction of the current which increases the efficiency and reliability of the motor. But, it still has some drawbacks such as high cost of permanent magnet on the rotor. Also the risk of demagnetization is draw back of PMSM.

Due to the lack of magnetic material recently, SRM is used for EV applications, and it has good features like wide speed range, cost of motor, and high starting torque. However, it still has problems like excessive noise, vibrations, and variations in torque while in use. Since the efficiency value is identical to IM over a wide speed range, the utilization rate in EVs low as compared to IM due to high torque fluctuations, which lead to high noise and vibrations [18]. Induction motors are preferred over other types of motors in EV applications due to their uniform air gap, durability, low cost, lack of demagnetization problems caused by temperature increases, and easily controllable features. [18].

Chapter 3

System Modeling and Tractive Force Model for Electric Vehicle

In this chapter, section 3.1 deals on modeling of the induction motor, and the result were verified in MATLAB Simulink under open-loop condition, and in section 3.2 states about tractive force model for EV application and load curve were developed in MATLAB Simulink.

3.1 Modeling of Induction Motor

The fundamental winding structure of the induction motor can be used to generate the mathematical model of the motor[2] considering that:

- All windings are sinusoidal distributions in space.
- The windings in the stator and the rotor are 120 degrees apart from each other.
- The stator and rotor winding are shifted by angle θ_r.

The voltage equation in abc reference frame will be [2].

$$V_{abcs} = r_s i_{abcs} + \frac{d\psi_{abcs}}{dt} \tag{3.1}$$

$$V_{abcr} = r_r i_{abcr} + \frac{d\psi_{abcr}}{dt} \tag{3.2}$$

Also, For a magnetically linear system, the flux linkages can be expressed as a

function of inductance and phase current as shown in the following array [30].

$$\begin{bmatrix} \psi_{abcs} \\ \\ \psi_{abcr} \end{bmatrix} = \begin{bmatrix} L_s & L_{sr} \\ \\ (L_{sr})^T & Lr \end{bmatrix} \begin{bmatrix} i_{abcs} \\ \\ i_{abcr} \end{bmatrix} \tag{3.3}$$

where

$$L_s = \begin{bmatrix} L_{ls} + L_m & -\frac{1}{2}L_m & -\frac{1}{2}L_m \\ -\frac{1}{2}L_m & L_{ls} + L_m & -\frac{1}{2}L_m \\ -\frac{1}{2}L_m & -\frac{1}{2}L_m & -\frac{1}{2}L_m \end{bmatrix} \tag{3.4}$$

$$L_r = \begin{bmatrix} L_{lr} + L_m & -\frac{1}{2}L_m & -\frac{1}{2}L_m \\ -\frac{1}{2}L_m & L_{lr} + L_m & -\frac{1}{2}L_m \\ -\frac{1}{2}L_m & -\frac{1}{2}L_m & L_{lr} + L_m \end{bmatrix} \tag{3.5}$$

$$L_{sr} = L_{sr} \begin{bmatrix} \cos\theta_r & \cos(\theta_r + \frac{2\pi}{3}) & \cos(\theta_r - \frac{2\pi}{3}) \\ \cos(\theta_r - \frac{2\pi}{3}) & \cos\theta_r & \cos(\theta_r + \frac{2\pi}{3}) \\ \cos(\theta_r + \frac{2\pi}{3}) & \cos(\theta_r - \frac{2\pi}{3}) & \cos(\theta_r) \end{bmatrix} \tag{3.6}$$

where, the inductance L_{sr} is the amplitude of the mutual inductance between the stator and rotor windings, and L_{ls},L_{lr}, and Lm stand for stator leakage inductance, rotor leakage inductance, and magnetizing inductance, respectively.

Assuming that the co-energy (Wc) and the stored energy (Wf) are equal, the electromechanical torque of an induction motor can be calculated using a linear relationship between flux linkage and current.[20][26].

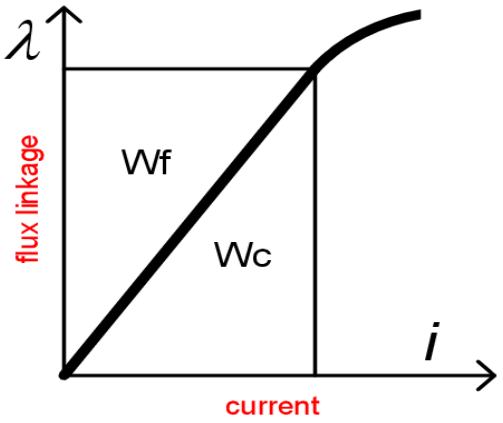

Figure 3.1: Stored energy and co-energy

The following formula provides the energy stored in the field between the mechanical and electrical systems:

$$W_f(i,\theta_r) = (\frac{1}{2})^n \sum_{p=1}^{J}\sum_{q=1}^{J} L_{pq} i_p i_q \Big|_{n=1\ p=q\ =0otherwise} \tag{3.7}$$

electromagnetic torque can be expressed as a function of the co-energy equation.

$$T_e(i_j,\theta_r) = \frac{p}{2}\frac{\alpha W_c(i_j,\theta_r)}{d\theta_r} \tag{3.8}$$

Since for linear system the energy and co-energy are equal.

$$T_e(i_j,\theta_r) = \frac{1}{2}(i_{abcs})^T \frac{\alpha}{\alpha\theta_r}[L'_{sr}]i'_{abcr} \tag{3.9}$$

- Since the above equations are non-linear and complex, they can be simplified by transforming them to a synchronously rotating reference frame. Where synchronous reference frame is when the speed of the reference frame is synchronous speed w_e.
- In reference frame theory, the phase variables are converted to equivalent variables in a given reference frame. So, simple and linear voltage and torque equations like that of DC machines can be obtained[13].

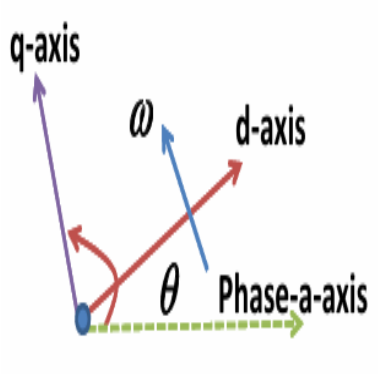

Figure 3.2: Rotating reference frame

where: $w = w_s$ synchronous speed, $\theta = \theta_s$ is the angle between the q-axis of the synchronously rotating reference frame and the stator phase a axis. Hence, $\frac{d\theta_s}{d_t} = w_s$, As a convention, q-axis is always ahead of d- axis by 90 degrees.

Let f_{abcs} be used to represent the three phase stator variables. V stands in for f if the variable is voltage, i for current, and ψ for flux linkage.

Similarly, let the transformed variables be represented by f. Now, the linear transformation of three variables should result three variables. The q-axis and d-axis components of the phase variables make up two of the three converted variables, and the zero component makes up the third. If the three phase variables are balanced system, then the zero component value is zero. The transformation takes place using the transformation matrix [2] K_s Like:.

$$f_{qd0s} = K_s f_{abcs} \tag{3.10}$$

$$f_{abcs} = K^{-1}{}_s f_{dq0s} \tag{3.11}$$

where K_s and K_s^{-1} is represented as:

$$K_s = \frac{2}{3}\begin{bmatrix} \cos\theta_s & \cos(\theta_s - \frac{2\pi}{3}) & \cos(\theta_s + \frac{2\pi}{3}) \\ \sin\theta_s & \sin(\theta_s - \frac{2\pi}{3}) & \sin(\theta_s + \frac{2\pi}{3}) \\ \frac{1}{2} & \frac{1}{2} & \frac{1}{2} \end{bmatrix} \qquad (K_s)^{-1} = \frac{2}{3}\begin{bmatrix} \cos\theta_s & \sin\theta_s & 1 \\ \cos(\theta_s - \frac{2\pi}{3}) & \sin(\theta_s - \frac{2\pi}{3}) & 1 \\ \cos(\theta_s + \frac{2\pi}{3}) & \sin(\theta_s + \frac{2\pi}{3}) & 1 \end{bmatrix} \tag{3.12}$$

So, in the synchronous rotating reference frame if the phases are sinusoidal and balanced, all variables become direct current.The transformed variable can be expressed in the following equivalent circuit.

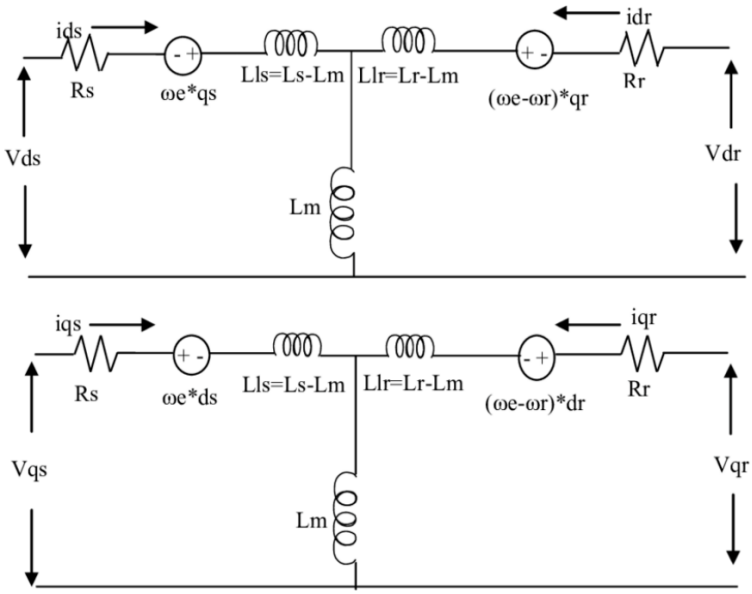

Figure 3.3: Equivalent circuit of Induction Motor

The motor's stator and rotor voltage equation can be expressed as a function of current and flux linkage using the equivalent circuit.[2] :

$$V_s = R_s I_s + \frac{d\psi_s}{dt} + jw_s\psi_s \tag{3.13}$$

$$V_r = R_r I_r + \frac{d\psi_r}{dt} - (w_s - w)\psi_r \tag{3.14}$$

where: $j = \begin{bmatrix} 0 & -1 \\ 1 & 0 \end{bmatrix}$

$V_s = \begin{bmatrix} V_{sd} & V_{sq} \end{bmatrix}^T$: stator voltage

$i_s = \begin{bmatrix} i_{sd} & i_{sq} \end{bmatrix}^T$; stator current

$i_r = \begin{bmatrix} i_{rd} & i_{rq} \end{bmatrix}^T$: rotor current

$\psi_s = \begin{bmatrix} \psi_{sd} & \psi_{sq} \end{bmatrix}^T$: stator flux linkage

$$\psi_r = \begin{bmatrix} \psi_{rd} & \psi_{rq} \end{bmatrix}^T \quad \text{: rotor flux linkage}$$

where w_s is the synchronous speed of the reference frame, R_r is the rotor resistance, w is the rotor speed, and R_s is the stator resistance.

$$\psi_s = L_s i_s + L_m i_r \tag{3.15}$$

$$\psi_r = L_m i_s + L_r i_r \tag{3.16}$$

where L_r is the rotor inductance, L_s is the stator inductance, and L_m is the mutual inductance. Additionally, the stator current and stator flux can be used to express the electric torque generated by the induction machine, such as

$$T_e = \frac{3}{2} p(\psi_s * i_s) \tag{3.17}$$

where p is the number of pole pairs.
By adjusting the aforementioned equations, the induction machine's electromagnetic behavior can be shown using state space equations as follows[14].

$$\dot{x} = Ax + Bu \tag{3.18}$$

$$y = Cx + Du \tag{3.19}$$

where, $x = \begin{bmatrix} i_{sd} & i_{sq} & \psi_{rd} & \psi_{rq} \end{bmatrix}^T$

$u = \begin{bmatrix} v_{sd} & v_{sq} \end{bmatrix}^T$ input variable

$y = \begin{bmatrix} i_{sd} & i_{sq} \end{bmatrix}^T$ output variable

Also, state-space matrices A, B, C and D expressed as:

$$A = \begin{bmatrix} -\frac{1}{\tau_\sigma} & w_s & \frac{k_r}{R_\sigma \tau_\sigma \tau_r} & \frac{k_r w}{R_\sigma \tau_\sigma} \\ -w_s & -\frac{1}{\tau\sigma} & -\frac{k_r w}{R_\sigma \tau_\sigma} & \frac{k_r}{R_\sigma \tau_\sigma \tau_r} \\ \frac{L_m}{\tau_r} & 0 & -\frac{1}{\tau_r} & -(w - w_s) \\ 0 & \frac{L_m}{\tau_r} & (w - w_s) & -\frac{1}{\tau_r} \end{bmatrix} \tag{3.20}$$

$$B = \begin{bmatrix} \frac{1}{\sigma L_s} & 0 \\ 0 & \frac{1}{\sigma L_s} \\ 0 & 0 \\ 0 & 0 \end{bmatrix} \tag{3.21}$$

$$C = \begin{bmatrix} 1 & 0 & 0 & 0 \\ 0 & 1 & 0 & 0 \end{bmatrix} \tag{3.22}$$

$$D = \begin{bmatrix} 0 & 0 \\ 0 & 0 \end{bmatrix} \tag{3.23}$$

where $k_r = \frac{L_m}{L_r}$, $\tau_r = \frac{L_r}{R_r}$, $\sigma = 1 - \frac{L_m^2}{L_s L_r}$, $R_\sigma = R_s + k_r^2 R_r$, and $\tau_\sigma = \sigma \frac{L_s}{R_\sigma}$.

Using the following motor parameter[36] the model of the motor were verified in MATLAB/Simulink:

Motor parameter	Specification
Rated Power	37 kw
Rated Speed	1480 rpm
Pole pair(p)	2
Rs	0.0851 Ω
Rr	0.0658 Ω
Ls	0.0314 H
Lr	0.0291 H
Lm	0.0291 H
Inertia (J)	0.37 kgm^2
Friction Factor (k_f)	0.02791 Nms

Table 3.1: Three-Phase Induction Motor Specification.

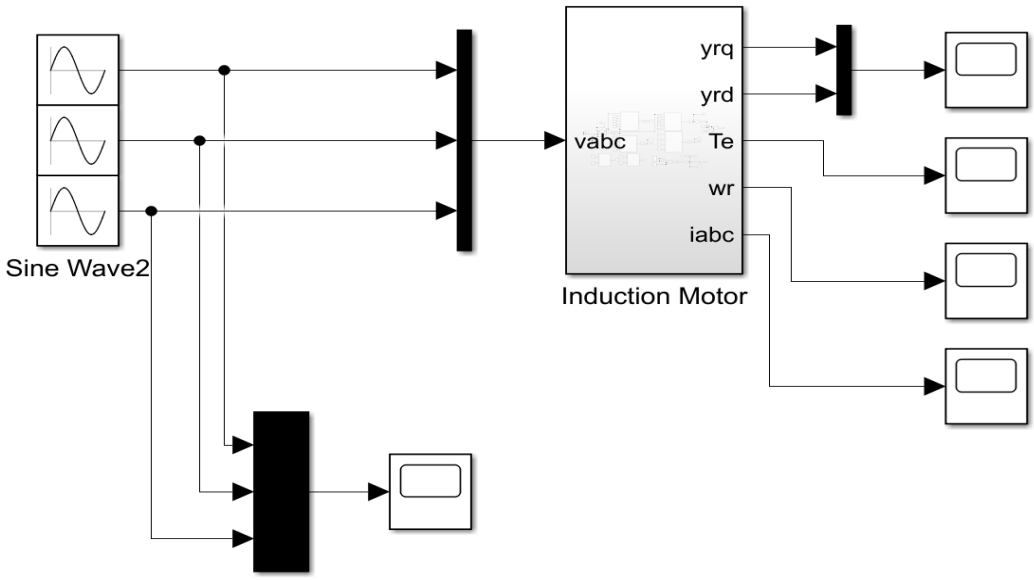

Figure 3.4: The overall Block Diagram for Model Verification

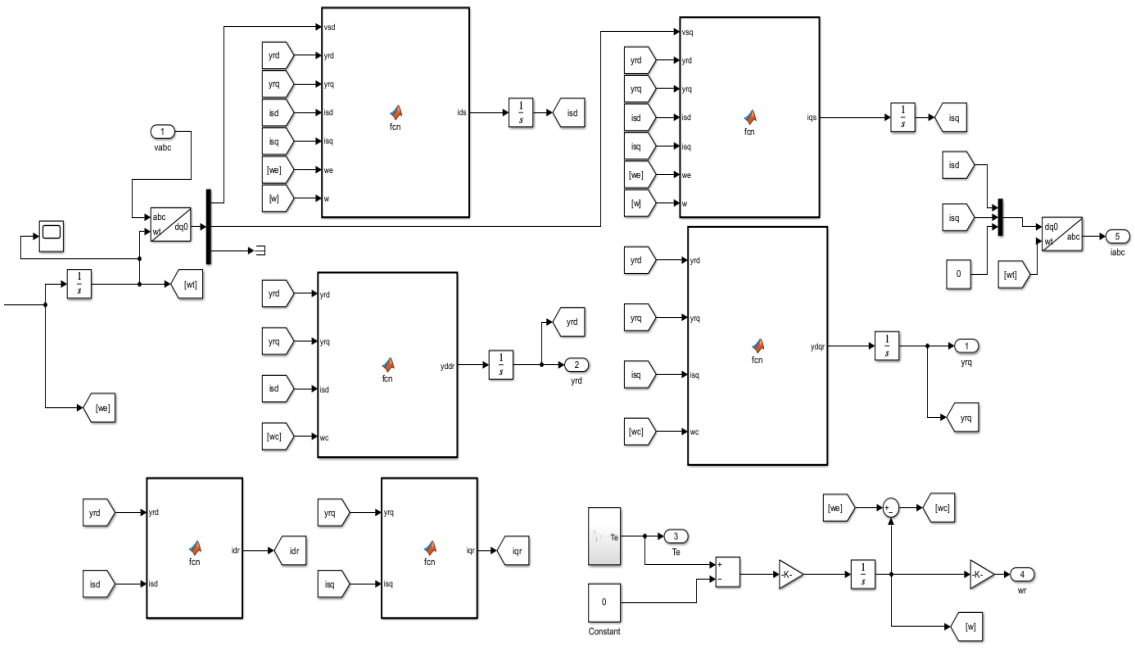

Figure 3.5: Induction Motor Simulink Model

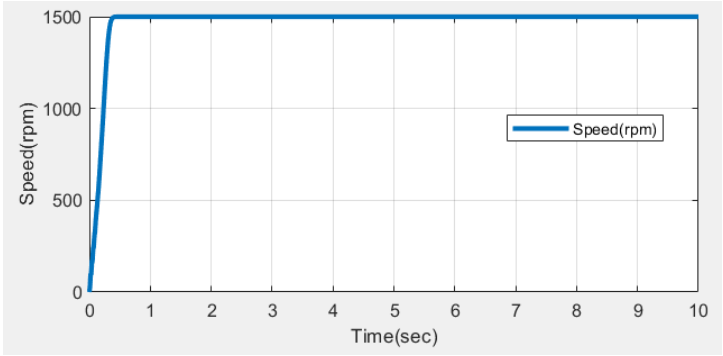

(a) Rotor Speed.

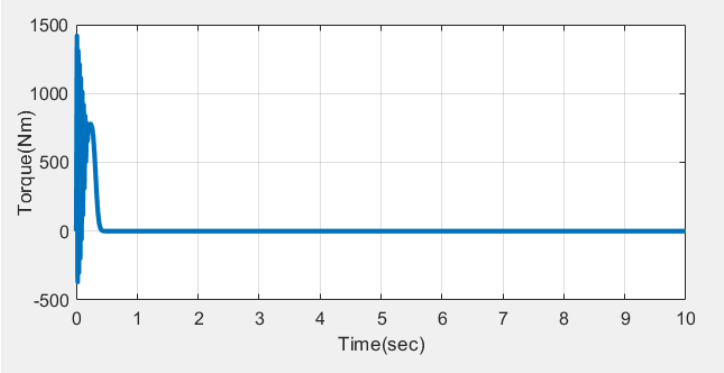

(b) Electro-magnetic torque.

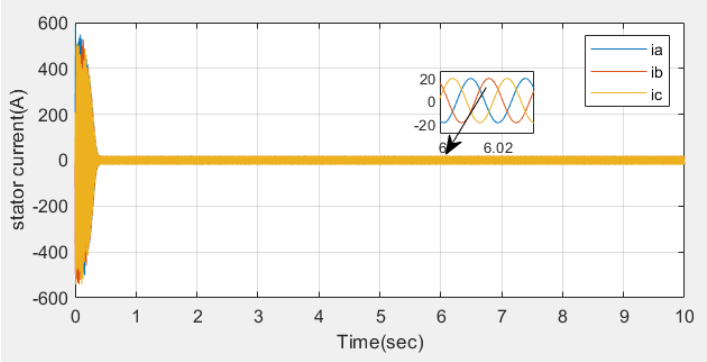

(c) Stator current.

Figure 3.6: Model verification result at no-load.

Since the machine is not loaded, the steady-state speed stabilizes at a value near the synchronism speed. The torque exhibits strong pulsation at no-load starting, peaking at about 3.2 times the nominal torque. This is caused by the noises produced by the mechanical component, and it tends toward the value that corresponds to the zero load once the transitory mode has vanished. At startup, the absorbed current is high—roughly three times the rated amount. The current that corresponds to the no-loaded motor's inductive behavior is still present at steady state. At startup, the rotor current is substantial, and at steady state, it completely disappears.

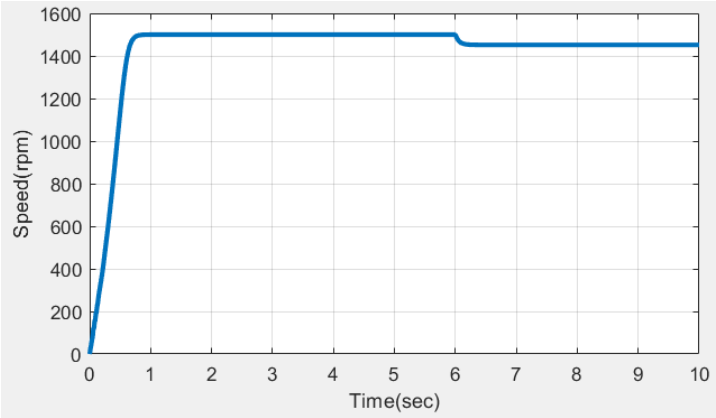

(a) Rotor Speed.

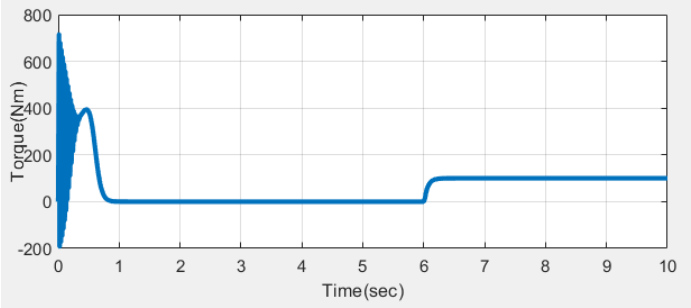

(b) Electro-magnetic torque.

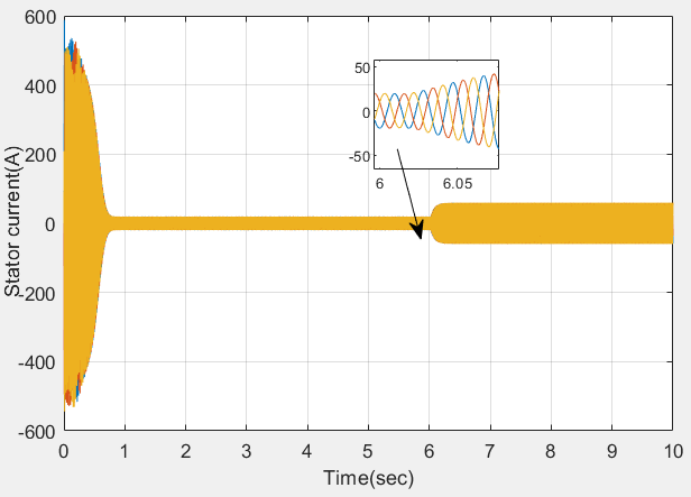

(c) Stator current.

Figure 3.7: Model verification result at $T_L = 100$ after $6sec$.

Under load: The machine shaft receives a load torque of TL = 100 (at time t=6 sec). The rotational speed clearly decreases when the electromagnetic torque equals the load torque. Also, as shown in figure 3.7 c the magnitude of the stator currents increases.

3.2 Tractive Force Calculation for Electric Vehicle

For traction applications, electric motors in electric vehicles must generate the necessary power and other qualities, such as high torque density, wide speed range, and high starting torque. Choosing the right motor rating based on the load to be carried is a crucial task. When choosing the right electric motor to supply the necessary power and torque for traction, vehicle dynamics are taken into account [29]. A vehicle's output characteristics, including power, torque, and speed, are determined by an electric motor.In order to overcome the force caused by the load and other opposing forces acting on the vehicle body, the electric motor used to drive the vehicle must be able to deliver enough power and torque.

This thesis used MAT-LAB/SIMULINK software to model a 500 kg weighted vehicle tractive force using an equation-based method at a rated speed. A few modeling parameters are extracted from the paper.[22]. This section's primary goal is to represent the vehicle on the road surface also, taking gradient resistance force into account. and the road load curve were plotted in Matlab/simulink environment. Also lookup table is used to describe load torque as a function of speed which is used as a disturbance for the motor.

Parameter	car
Vehicle mass(m)	500 kg
Radius of the wheel(r)	0.279m
Rolling resistance coefficient(C_{rr})	0.02
Gravitational acceleration(g)	9.8m/s^2
Distance from front axis to centroid	1.4m
Distance from rear axis to centroid	1.6m
Center of gravity height from the ground	0.5m
Frontal area(A)	1.2m^2
Air drag co-efficient(cd)	0.4
Air density(ρ)	1.2Kg/m^3
using velocity of the vehicle(V)	16.67m/s

Table 3.2: Parameters used for vehicle modeling

[32], states that the road load equation consists of the tires rolling resistance(F_{rr}), aerodynamic drag force (F_{ad}) acceleration force (F_a), and gradient force(F_{hc}). To move the vehicle forward at the intended speed, the motor must over come the total tractive force expressed as.

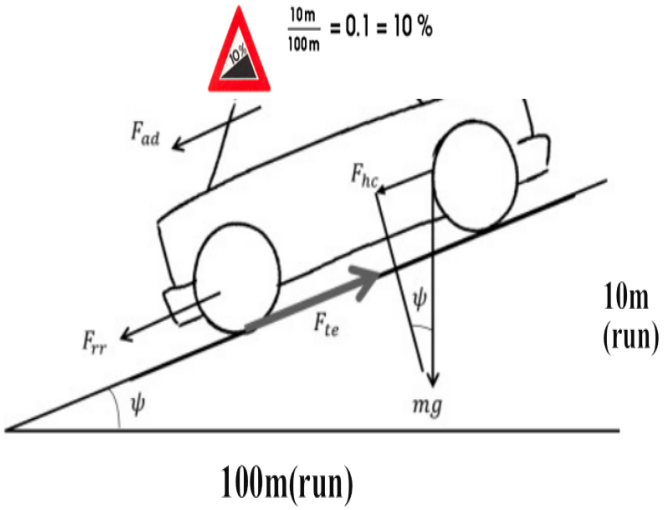

Figure 3.8: Elementary forces acting on a vehicle.

$$F_{te} = F_{rr} + F_{hc} + F_{ad} + F_a \tag{3.24}$$

- The resistance force that the vehicle experiences as a result of the tires' contact with the road is known as rolling resistance force and it can be expressed as:

$$F_{rr} = C_{rr} * m * g = 0.02 * 500 * 9.8 = 98N \tag{3.25}$$

- The resistant force provided by the air acting on the vehicle body is known as the aerodynamic drag force. The vehicle's shape has a major influence. Mathematically expressed as:

$$F_{ad} = 0.5 * \rho * C_d * A * V^2 = 80.03N \tag{3.26}$$

- The force that helps a vehicle accelerate from rest to a steady state speed in a predetermined amount of time is known as the acceleration force. There is a direct correlation between the acceleration force and the motor torque. Greater torque reduces the amount of time the car needs to reach a certain speed. The vehicle's mass determines the acceleration force as shown below. [5].

$$F_a = ma \tag{3.27}$$

$$a = \frac{V - V_o}{t_f - t_o} \tag{3.28}$$

Using the above equation the vehicle's acceleration computed considering that it reaches its steady state speed in ten seconds and the obtained acceleration is $835N$.

- gradient force: in an electric vehicle refers to the force acting on the vehicle when it is driving uphill or downhill, essentially the component of gravity pulling the vehicle along the slope of the road, which is directly related to the inclination angle of the road surface; meaning it is a force that either assists the vehicle when going downhill or opposes it when going uphill[5]. assuming that the angle of inclination is 0.0997 in radian.

$$F_{hc} = mgsin(\alpha) = 487.72 \tag{3.29}$$

$$F_{te} = F_a + F_{ad} + F_{hc} + F_{rr} \tag{3.30}$$

$$F_{te} = 835 + 80.03 + 487.72 + 98 = 1500.75N \tag{3.31}$$

So the amount of power needed to move the car at a specific speed would be;

$$P_t = F_{te} * V = 1500.75 * 16.67 = 25.02kw \tag{3.32}$$

Since, the power rating of the proposed motor is 37kw as shown in the above value it can overcome the ev load.

Also, the total traction torque T_{te} is given by

$$T_{te} = T_L = F_{te}\frac{r}{G} \tag{3.33}$$

where, r and G are radius of the wheel and gear ratio respectively.

3.2.1 Tractive Force Vs Speed Curve in MATLAB/SIMULINK Environment

In order to show the relationship between the speed and tractive force based on the above mathematical equation the load curve were plotted in matlab/simulik environment using vehicle parameters in 3.1 as shown in the below figure:

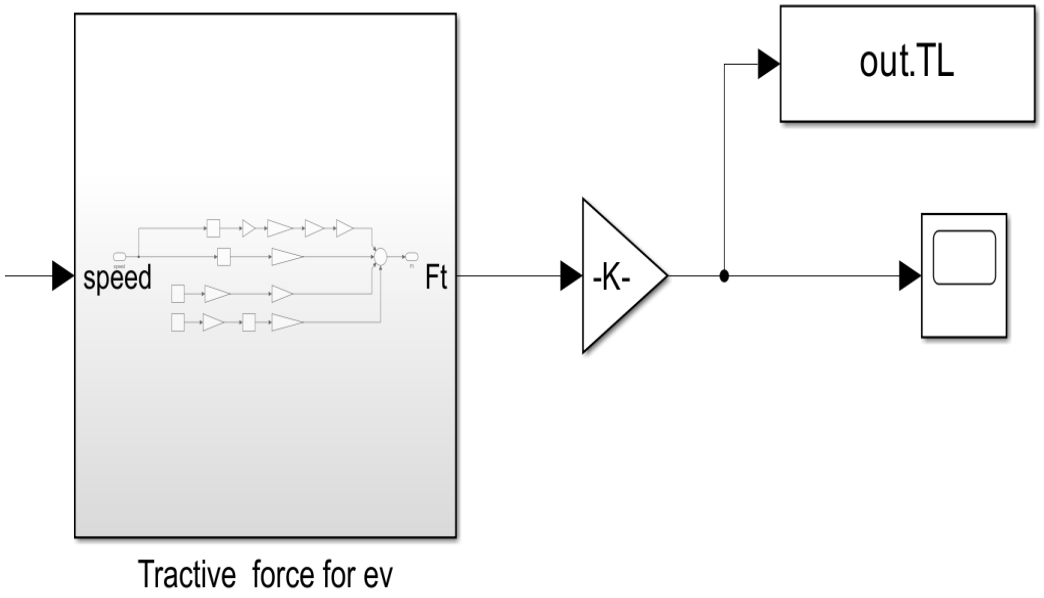

Figure 3.9: Tractive force simulink model for ev

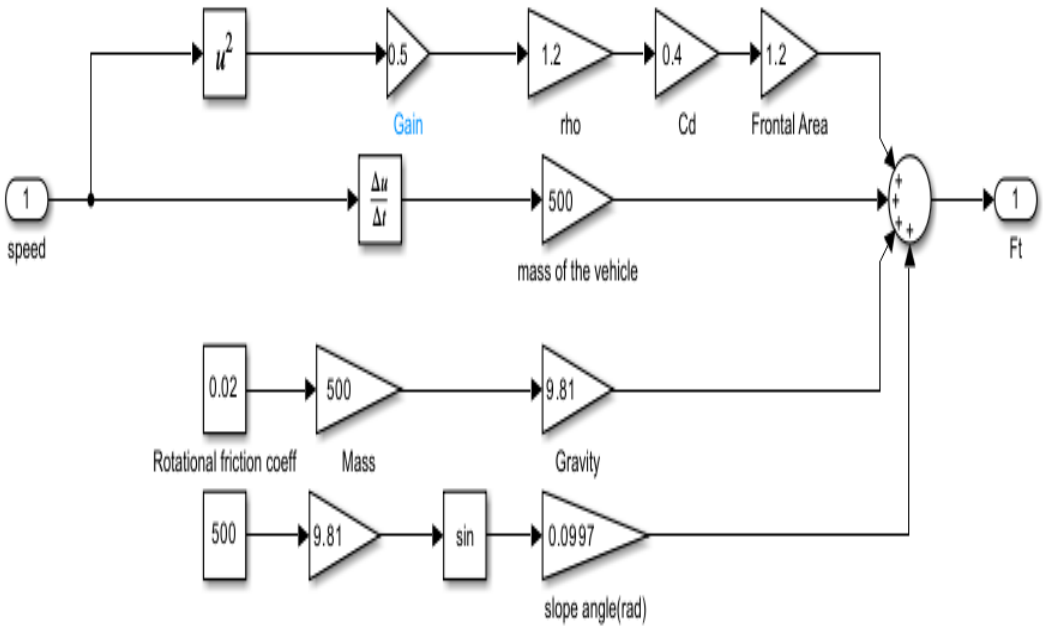

Figure 3.10: Inside the tractive force block

A road load curve is a graphical or mathematical representation of the overall resistive forces (or power) at different speeds that a vehicle must overcome to counteract drag, rolling resistance, and other forces in order to continue moving. It is necessary for auto manufacturers and government agencies to conduct real-world driving on a dynamometer for fuel economy and emissions testing, using the road load curve to replicate the resistance the vehicle would encounter while driving on the road.The load curve were plotted in matlab simulink and as shown in the following figure considering 10% steeper road:

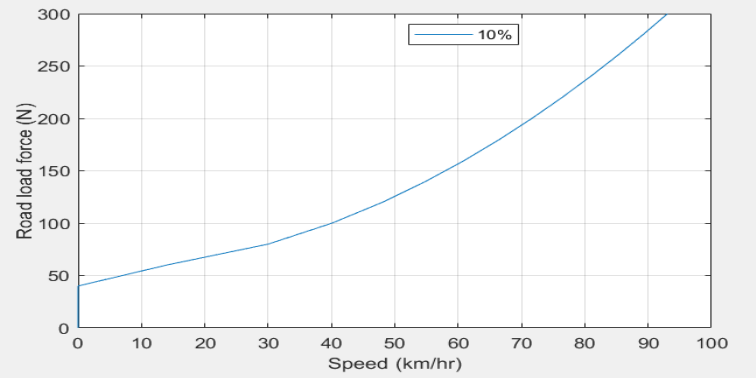

Figure 3.11: Road load curve

Chapter 4

Control Techniques

This chapter deals with controller design for the system.In this thesis, a cascaded control structure is used, which has an external loop and internal loop. Where the external loop is used for controlling the speed of the motor, and its result verified through non-linear mpc, integral sliding mode control(ISMC) and lqr controllers. Using the finite control set model predictive torque control (FCS-MPTC) technique, the inner part controls the motor's torque.

4.1 Model Predictive Control

Uncontrolled operation of induction motors will result in high output parameter (speed and torque) inaccuracy, and low dynamic responsiveness. Model Predictive Control (MPC) is a popular control technique in modern drive control systems. In a control system, the controller's objective is to select the plant's input such that, within a specified time frame, the plant's output complies with the intended reference. Using the system model, MPC predicts the next plant output. Additionally, it makes use of an optimizer to guarantee that the predicted future plant output follows the intended reference.

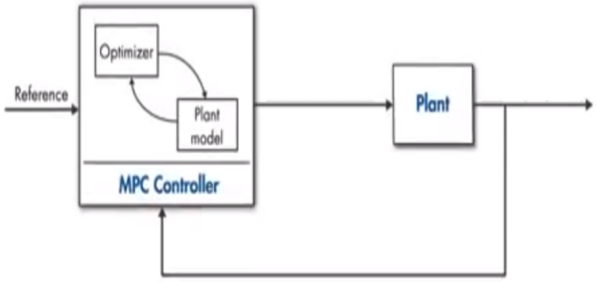

Figure 4.1: Block Diagram of MPC

It calculates the optimal control inputs in relation to a specified control objective and system constraints using the plant's predicted, and estimated states.

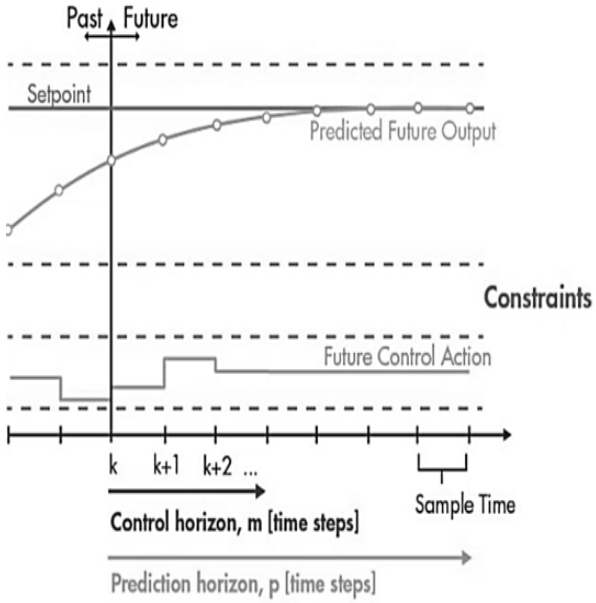

Figure 4.2: Graphical representation of MPC

Let's assume that the vertical axis represents the current time, the value behind it represents the past, and the value on the right represents the future in order to quickly comprehend the MPC's operation as seen in the image above. In order to track the speed's reference for the upcoming p (prediction horizon) time, MPC currently uses the speed model to simulate the speed's path. This illustrates how far ahead MPC looks. Let's use a system to provide more context.

$$x(k+1) = f(x(k), u(k)) \tag{4.1}$$

where u is a control action and x is the state. At time k measure the state of $x(k)$ based

on that $x(k)$ compute the optimal sequence of control action over the prediction horizon.

$$u(x(k)) = (u(k), u(k+1), ...u(k+p-1)) \tag{4.2}$$

At the subsequent decision moment mpc applies the control input $u(k)$ over the sampling interval [k,k+1] it repeats the same processes over the prediction horizon. In general in mpc prediction is used to determine how the state x changes over the horizon, To reduce the discrepancy between the reference and predicted states, online optimization is utilized. by utilizing control actions, and receding horizon implementation is required at each sample period until the reference is reached (over the prediction horizon) [24].

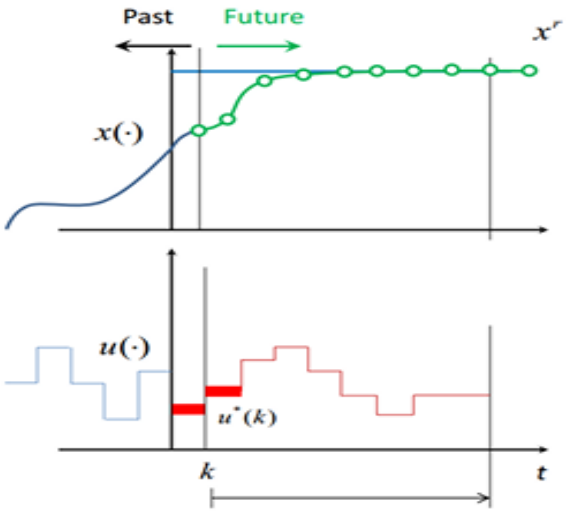

Figure 4.3: receding horizon implementation

The MPC parameters have an impact on the controller's performance as well as the computational complexity of the MPC method, which solves an online optimization problem, at each time step. As a result, selecting appropriate MPC parameter values at each time step is crucial. The following is a mathematical formulation of MPC[24]:

$$J(x,u) = \sum_{k=0}^{P} (x_p - x_r)^T * Q * (x_p - x_r) + (u(k)^T * R * u(k)) \tag{4.3}$$

where p is the prediction horizon

$$
\begin{aligned}
s.t \quad & x(k+1) = f(x(k), u(k)) \\
& x(k) \in x, \forall \in [0, p] \\
& u(k) \in U, \forall \in [0, N]
\end{aligned} \tag{4.4}
$$

Achieving optimal controller performance and reducing the computational complexity of mpc algorithms that performs online optimization problems at each time depend on selecting the appropriate value for the mpc parameter[31]. In addition, there is a recommendation on choosing the controller prediction and control horizon, constraints, and sample time. It is advised to select 10 to 20 samples during the open-loop system response's rise time. It is well known that the MPC controller predicts future plant output, and the optimizer determines the best control input sequence to bring the predicted plant output as close to the set-point as possible. The prediction horizon, which indicates how far into the future the controller predicts, is the number of predicted future time steps. It is advised to use 20 to 30 open-loop transient response samples when selecting the prediction horizon. Because of the computational complexity, it is advised to select a control horizon of two to three steps, with 10 to 20 percent of the prediction horizon.

4.1.1 Non-Linear Model Predictive Speed Control of IM

Non-linear mpc uses a combination of constrained optimization and model-based prediction to determine control actions at each control interval. In non-linear model predictive controller, it needs to convert the OCP 4.3 to the NLP. So, to do that, there are different methods like single shooting and multiple shooting. In single shooting only the manipulated variables are used for the control action but In multiple shooting both the state and manipulated variable used as a decision variable which has fast and good performance. nonlinear programming problem described as[24]:

$$
\min_{z} \phi(z), \quad (objective\, function) \tag{4.5}
$$

$$
s.t \quad g(z) = 0, \tag{4.6}
$$

where $\phi(z)$ are object function , decision variable z, and constraints, which may be equality $g(z)$ equality constraints. By default, nonlinear mpc controllers requires an optimization toolbox license to solve a nonlinear programming problem using the fmincon function with the sqp algorithm. Also, it uses a multiple-shooting method to convert OCP to NLP. In this method both the state and manipulated variable used as a decision variable.

In this paper to control a non-linear speed dynamics of induction motor non-linear mpc block is used from model predictive toolbox. To use the block non-linear mpc object were created in Matlab script and specified it in the block dialog. Nonlinear mpc controller was designed and its parameter defined on the script as shown in the appendix part of the thesis and also in order to control the speed of the motor casadi(tool for nonlinear optimization) is used at $500rpm$ and $40Nm$ load torque.
In this thesis the speed of the induction motor is controlled in order to track its desired reference. Using the speed of the motor as state variable $w_r(t) = x(t)$

$$\dot{x(t)} = Ax(t) + Bu(t) + d \tag{4.7}$$

$$\dot{w_r(t)} = \frac{1}{J}(-k_f w_r(t) + T_e(t) - T_L) \tag{4.8}$$

$$\dot{x(t)} = \frac{1}{J}(-k_f x(t) + T_e(t) - T_L) \tag{4.9}$$

where k_f is friction factor, J is inertia, T_e is electromagnetic torque used as manipulated variable, T_L is load torque which used as measured disturbance in the motor, and w_r is the motor speed.

Also, forward Euler discretization technique is used in order to predict the future output or the next step.

$$\frac{dx}{dt} = \frac{x(k+1) - x(k)}{T_s} \tag{4.10}$$

where, T_s is sample period

4.2 Finite Control Set Model Predictive Torque Control (FCS-MPTC)

FCS-MPTC has recently become popular for the drives of induction motors due to its ease of structure and flexibility to incorporate additional control parameters into the control law. The control system of FCS-MPTC has three parts, which are estimation, prediction, and optimization. Initially, the motor fluxes linkage(rotor and stator) instantaneous values are estimated. Then the prediction of torque and flux is done. Finally, the vector that best satisfies the control objectives is identified as the optimum voltage vector. The estimation block for the current instant (k) evaluates machine parameters that cannot be measured, such as the rotor flux $\psi_r(k)$ and stator flux $\psi_s(k)$. Eight flux values and eight torque values are generated for the (k + 1)th instant using the estimated and measured motor parameter at instant k. The prediction block calculates (k +1)th instant flux

and torque for all possible switching combinations of the inverter, of which six of them are active voltage vectors and remaining two are null vectors of 2-level VSI. These eight (k + 1)th instant values are compared to the reference torque and flux in the cost minimization block. For the (k + 1)th instant, the inverter is subjected to the voltage vector switching sequence that provides the lowest flux error and torque error[4].

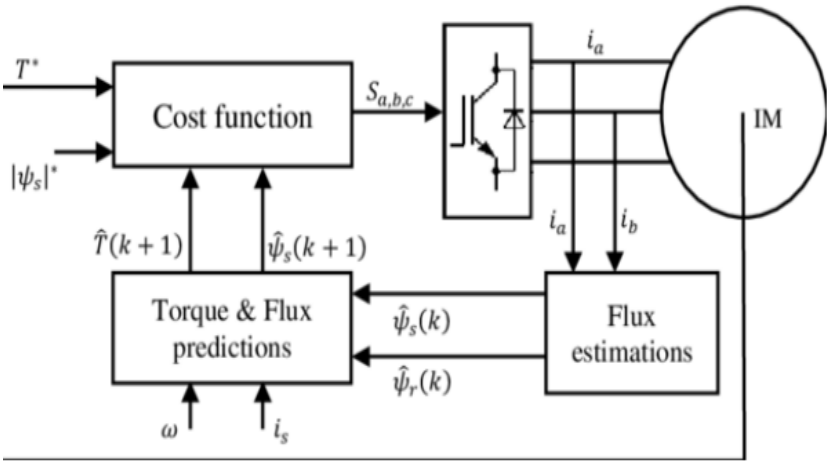

Figure 4.4: FCS-MPTC Block Diagram

The Overall Control Technique of FCS-MPTC

To estimate, predict, and optimize the cost function in the controller design process, this control technique uses torque and flux as control parameters. [4].

1. Rotor Flux and Stator Flux Estimation

   The estimation of rotor and stator flux is the first step in PTC design, as seen in 4.4 . So, to do that at the stationary reference frame, the stator voltage equation expressed as:

$$V_s = R_s I_s + \frac{d\psi_s}{dt} \tag{4.11}$$

   Using equation 4.12 stator flux is estimated as,

$$\frac{d\psi_s}{dt} = V_S - R_S I_s \tag{4.12}$$

Rotor flux using equation.

$$\psi_r = (L_r I_r + L_m I_s) \tag{4.13}$$

where,

$$I_r = \frac{\psi_s - L_s I_s}{L_m} \tag{4.14}$$

So, the estimated rotor flux is obtained substituting equation 4.14 into equation 4.13.

$$\psi_r = (\frac{L_m}{L_r}\psi_s + I_s(L_m - (\frac{L_r L_s}{L_m})) \tag{4.15}$$

using back ward euler discretization technique the equation 4.12 and 4.15 can be written in discrete format as:

$$\psi_s(k) = \psi_s(k-1) + T_s[V_s(k-1) - R_s i_s(k-1)] \tag{4.16}$$

$$\psi_r(k) = (\frac{L_r}{L_m}\psi_s(k) + I_s(k-1)(L_m - (\frac{L_r L_s}{L_m})) \tag{4.17}$$

2. Torque and Flux Prediction
   Utilizing forward Euler discretizations, the necessary signals (current, flux, and torque) are predicted into the next step [1].

$$\frac{dx}{dt} = \frac{x(k+1) - x(k)}{T_s} \tag{4.18}$$

   T_s stands for sampling period.
   The required prediction of the control technique obtained from the above equation and expressed as prediction one period in the future as follow:

$$\psi_s(k+1) = \psi_s(k) + T_s V_S(k) - R_s T_s I_s(k) \tag{4.19}$$

$$i_s(k+1) = (1 - \frac{T_s}{\tau_\sigma})i_s(k) + \frac{T_s}{\tau_\sigma}\frac{1}{R_\sigma}[k_r(\frac{1}{T_r} - jw(k))\psi_r(k) + v_s(k)] \tag{4.20}$$

$$T_e(k+1) = \frac{3}{2}p \times imag[\psi_s(k+1) \cdot i_s(k+1)] \tag{4.21}$$

3. Cost Function Optimization
   Next, the cost function is stated as a function of torque and flux linkage error equa-

tion as follows:

$$g = \sum_{h=1}^{N} |T_e^*(k) - T_e(k+h)| + \lambda||\psi_s|^* - |\psi_s(k+h)|| \tag{4.22}$$

where h is the prediction horizon and in this instance, it is one, meaning that it see one period over the future horizon. λ is waiting factor set as the quotient of electromagnetic torque and rated stator flux.

The over all model of PTC will described in the following chart.

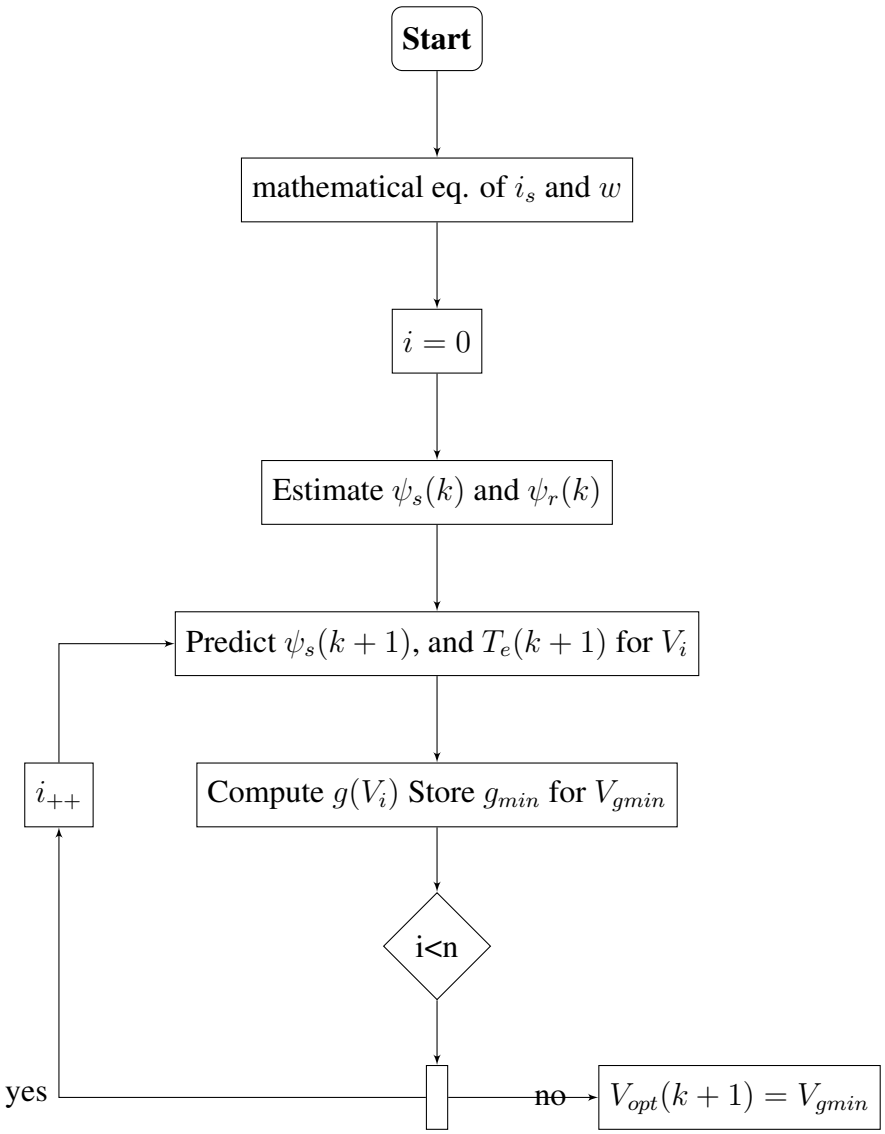

Figure 4.5: FCS-MPC Flowchart

From the above flowchart the overall algorithm of predictive torque controller are described as

- Initially the stator and the rotor flux is estimated as mentioned in the above.

- Then, using the motor model to predict motor parameters like torque and stator flux linkage for the next sampling period.
- Finally, the minimum cost function is computed from 6 active switching state of the inverter.

As describes in chapter two the switching sate of an 2L-VSI can be represented as:

$$S = \frac{2}{3}(S_a + e^{j2\pi/3}.S_b + e^{j4\pi/3}.S_c) \tag{4.23}$$

where S_a, S_b, S_c represented switching state of inverter. the output voltage vector can be written in a stationary frame as follows,

$$Vs = vdc.S \tag{4.24}$$

as seen in the image below Switching states can be used to represent the inverter's switches' operational status. For three phases, there are eight possible switching states because each phase has two possible switching states. In the stationary $(\alpha - \beta)$reference frame, every switching state generates a corresponding voltage vector. Two of those eight switching states $[111]$ and $[000]$ are zero states, while the remaining states are active.

V_i	$S = \{S_a S_b S_c\}$	$V_s = V_\alpha + jV_\beta$
V_0	000	0
V_1	100	$^2/_3\, V_{DC}$
V_2	110	$\left(^1/_3 + j\, ^1/_{\sqrt{3}}\right) V_{DC}$
V_3	010	$\left(^{-1}/_3 + j\, ^1/_{\sqrt{3}}\right) V_{DC}$
V_4	011	$^{-2}/_3\, V_{DC}$
V_5	001	$\left(^{-1}/_3 - j\, ^1/_{\sqrt{3}}\right) V_{DC}$
V_6	101	$\left(^1/_3 - j\, ^1/_{\sqrt{3}}\right) V_{DC}$
V_7	111	0

Figure 4.6: Switching state of 2L-VSI

4.3 LQR Design for Induction Motor

As, model predictive control a linear quadratic regulator (LQR) is an optimal control system widely used in control theory. It provides a systematic way to design feedback controllers for linear dynamic systems by minimizing a cost function. It is designed to operate linear dynamic systems optimally by minimizing a cost function that typically represents a trade-off between state performance and control effort.

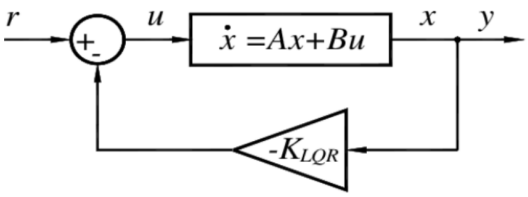

Figure 4.7: Block diagram of lqr controller

The controller's goal is to minimize the cost function while taking the state equation into consideration.[35].

$$J = \int_0^\infty x^T Q x + u^T R u \, dt \tag{4.25}$$

s.t

$$\dot{x} = Ax + Bu \tag{4.26}$$

The control action will be

$$U = -kx \tag{4.27}$$

where k is:

$$k = \frac{1}{R} B^T p \tag{4.28}$$

where p obtained from algebraic riccati equation,

$$A^T p + pA + Q - pB\frac{1}{R}B^T p = 0 \tag{4.29}$$

where R is a positive-definite and Q is a positive-semi-definite real symmetric weightings chosen by the design engineer. The closed-loop system will react differently depending on how these design parameters are chosen. In general, choosing a big Q indicates that the state x (t) is more penalized than the controller input u (t) to maintain a smaller cost function, or vice versa[35].

This indicates that higher values of Q typically cause the closed-loop system's poles, $Ac = (A - BK)$, to be more to the left in the s-plane, accelerating the state's decay to zero. Larger R, on the other hand, indicates that less control effort is used, which leads to

slower poles and higher state x(t) values.

The statement that Q must be positive semi-definite and R must be positive definite implies that for all functions x(t), the scalar number $x^T Qx$ is always positive or zero at time t, and for all values of u(t), the scalar quantity $u^T Ru$ is always positive at time t. This ensures that J is well defined[35].

In General to summarize the procedure taken on designing of lqr controller:

- First A and B values are taken from the plant state equation.
- Next design parameters Q and R are chosen..
- Then figure out p using the algebraic Riccati equation.
- Lastly, use 4.28 to determine the controller gain.

Using the Matlab command that minimizes a cost function with manually adjusted weighting factors, LQR is suggested in this thesis to control the induction motor's speed and the controller gain k.

using this angular speed equation as state space equation of induction motor at zero load torque the controller gain k were computed using matlab command and the result were verified in matlab simulink:

$$\frac{dw_r(t)}{dt} = \frac{1}{J}(-k_f w_r(t) + T_e(t)) \tag{4.30}$$

where k_f is frictional coefficient, j is inertia, $T_e$is electromagnetic torque used as control action, and w_r is a state variable.

4.4 Integral Sliding Mode Speed Control of Induction Motor

For induction motors, Integral Sliding Mode Control (ISMC) is a reliable control technique that can be used to improve performance even in the face of uncertainties and disturbance[7]. In this thesis ISMC were designed to control speed of the motor and the result were verified in matlab simulink and compared with the proposed mpc controller as shown bellow.

choosing the sliding surface s as:

$$s = e + \lambda \int e d_t \tag{4.31}$$

where, e is the error(the difference between the actual and reference speed), λ is the positive constant that determines the speed convergence Also, Lyapunov function V for stability criteria described as.

$$v = \frac{1}{2} s^2 \tag{4.32}$$

Since we have overall controller u is the sum of discontinuous controller (u_{dis}) which used to remove chattering from the sliding surface and equivalent controller (u_{eq}) expressed as.

$$u = u_{dis} + u_{eq} \tag{4.33}$$

u_{eq} can be found using:

$$u_{eq} = \frac{ds}{dt} = \dot{s} = 0 \tag{4.34}$$

also u_{dis} expressed as:

$$u_{dis} = ksign(s) \tag{4.35}$$

where k is positive constant which determined using Lyapunov stability criteria as:

$$\frac{dv}{dt} = s\dot{s} = 0 \tag{4.36}$$

So, in general to design ISMC in order to control speed of induction motor:

- The sliding surface and its derivative defined as:

$$s = e + \lambda \int e d_t \tag{4.37}$$

$$\dot{s} = \dot{e} + \lambda e \tag{4.38}$$

- The error e function will be:

$$e = w_r - w_{ref} \tag{4.39}$$

$$\dot{e} = \dot{w}_r \tag{4.40}$$

since w_{ref} is constant its derivative become zero where w_r is actual rotor speed of the motor and w_{ref} is the reference speed.
using state space speed equation of the IM $\dot{w_r}(t)$ described as:

$$\dot{w}_r = \frac{1}{J}(T_e - T_L) \tag{4.41}$$

using equation 4.34 and 4.38 to find u_{eq} choosing electromagnetic torque (T_e) as as equivalent controller as:

$$u_{eq} = T_e = -J\lambda(w_r - w_{ref}) + T_L \tag{4.42}$$

since the over all controller u is the summation of u_{eq} and u_{dis} as stated in equation 4.33 it becomes:

$$u = ksign(s) + J\lambda(w_r - w_{ref}) + T_L \tag{4.43}$$

- In order to find k using Lyapunov stability criteria using equation 4.45

$$\frac{dv}{dt} = s\dot{s} < 0 \tag{4.44}$$

$$= s[\frac{1}{J}(ksign(s))] < 0 \tag{4.45}$$

  - if $s < 0 \rightarrow sign(s) < 0, then\ \dot{v} < 0 \rightarrow k < 0$
  - if $s > 0 \rightarrow sign(s) > 0, then\ \dot{v} < 0 \rightarrow k < 0$

  Using the above value, the range of k is < 0. assuming $k = -1$ equation 4.43 becomes:

$$u = -sign(s) - J\lambda(w_r - w_{ref}) + T_L \tag{4.46}$$

  Therefore, the performance of the controller was verified in Matlab Simulink using the aforementioned control inputs4.46.

Chapter 5

Simulation Results and Discussion

To examine the predictive torque control system of an induction motor for EV applications, a mathematical model of the system was developed in the Matlab/Simulink environment. Tables 3.1 and 3.2 provide the motor and ev parameters used in the simulation, respectively. In this paper, torque and flux were controlled using the FCS-MPTC mechanism, and the motor's speed was managed by a nonlinear mpc controller. Also, ISMC and lqr controllers were used for a comparison purpose.

5.1 MPC and ISMC speed controller results considering vehicle inertia

The proposed controller performance was tested using the vehicle tractive force to generate load torque, which was then shown in a lookup table as a function of speed of the motor and sent back to the motor as a measured disturbance; the results were as follows:

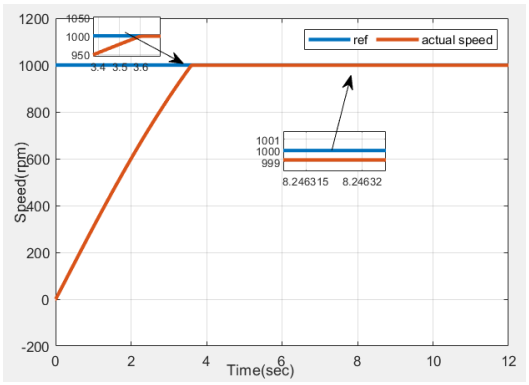

(a) motor speed result.

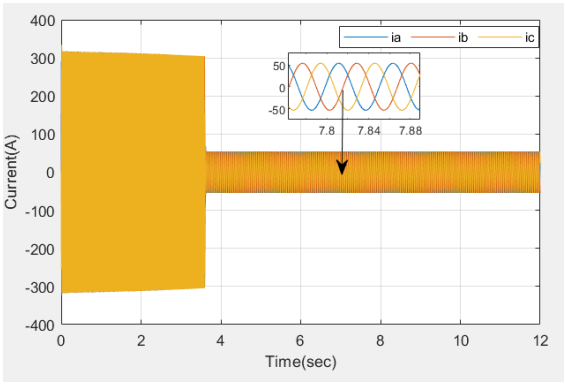

(b) stator current result.

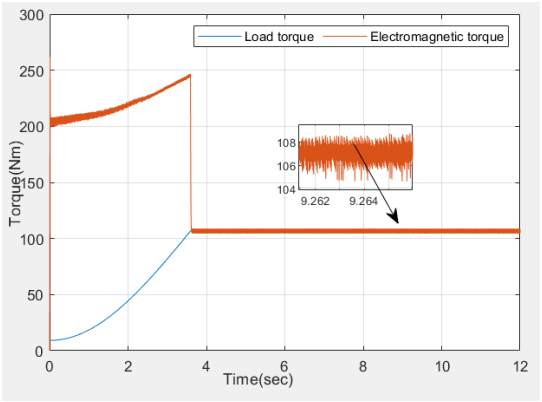

(c) electromagnetic torque result.

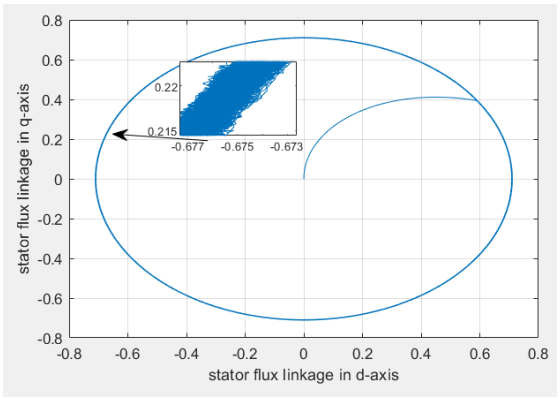

(d) flux circular trajectory result.

Figure 5.1: Performance of ISMC controller @1000rpm speed command.

Figure 5.1 shows the performance of Integral Sliding Mode speed controller results using tractive force load for ev as a disturbance to the motor through lookup table and as shown 5.1(a) the motor speed tracks its desired reference around $3.6sec$ with 0.01% steady state error and as figure 5.1(b) shows the starting current of three-phase induction motor is much higher than its full-load current. According figure 5.1(c) at starting the motor operates at maximum torque until it reaches the desired load torque since in this thesis PTC mechanism is used in order to control the torque of the motor the ripple effect much depends on the on the weighting factor λ. So, through adjustment much better result can be obtained and the circular trajectory of magnetic flux on figure 5.1(c) shows the rotating magnetic field produced by the stator windings.

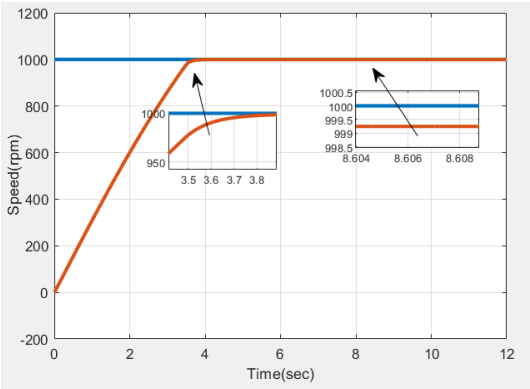

(a) motor speed result.

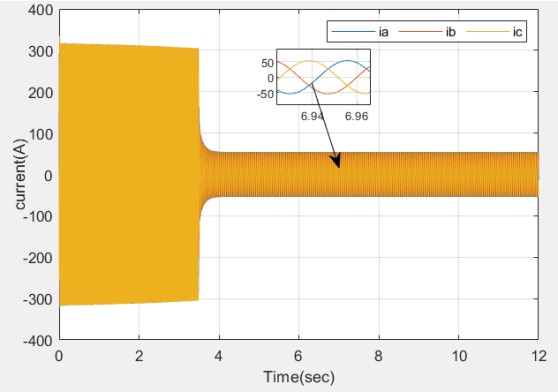

(b) stator current result.

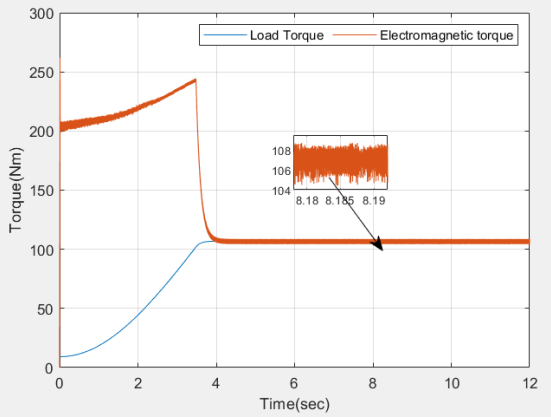

(c) electromagnetic torque result.

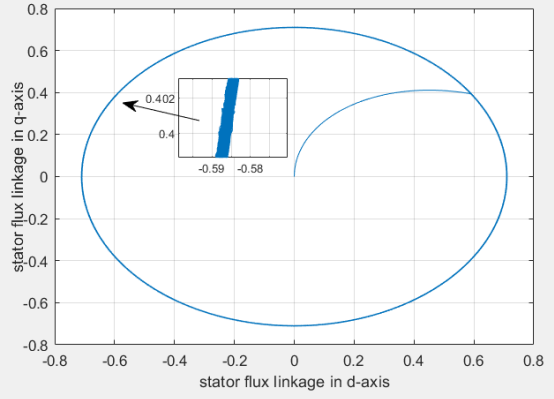

(d) flux circular trajectory result.

Figure 5.2: Performance of non-linear MPC controller @1000rpm speed command.

The results on figure 5.2 are based on MPC controller using tractive force load as a disturbance to the motor. as shown on figure 5.2(a) the actual speed track its desired reference at $3.7sec$ and with error of 0.008%.

In general, as shown in the above results, both MPC and ISMC have good performance (almost equivalent) in handling EV loads. So, it's recommended to use both controllers interchangeably.

5.2 Comparing the Performance of ISMC, LQR, and MPC Considering Constant Disturbance

With a reference speed of 500 RPM and a constant load torque of Tl = 40 Nm, the induction motor drive was contrasted with LQR, ISMC, and MPC (using Casadi) speed controllers. According to the simulation result displayed in figure 5.3, the mpc performs better dynamically than the lqr and slightly better than the ISMC controller. As can be seen in the zoomed-in portion of figure 5.3, the lqr controller has lower dynamic performance than others. Also, the steady-state error of the mpc speed controller is 0.0004%, ISMC speed controller is -0. 0014%, and the lqr speed controller is 0. 025% which shows that mpc performs better compared to others.

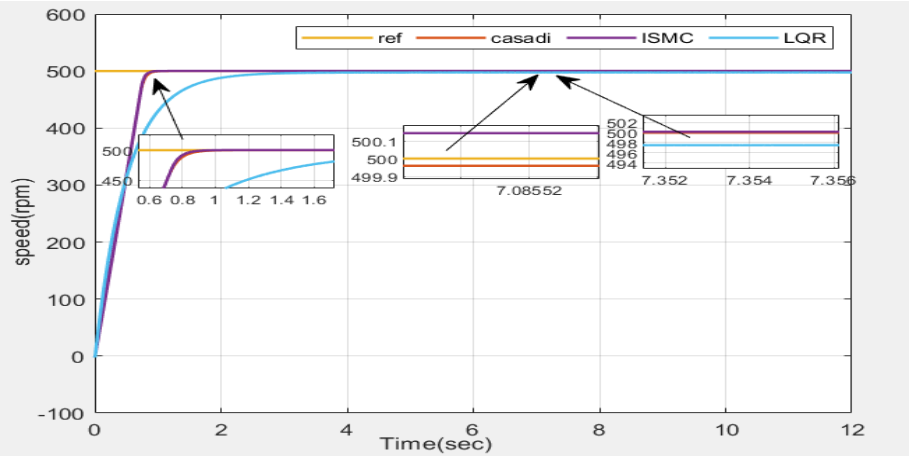

Figure 5.3: Speed Tracking Performance Comparison

5.3 MPC, ISMC, and LQR speed controller result

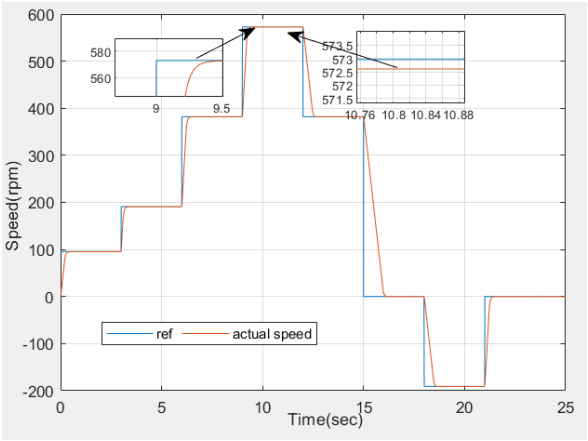

(a) motor speed result.

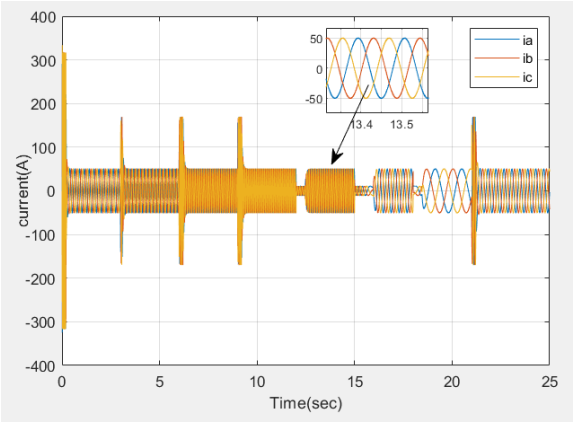

(b) stator current result.

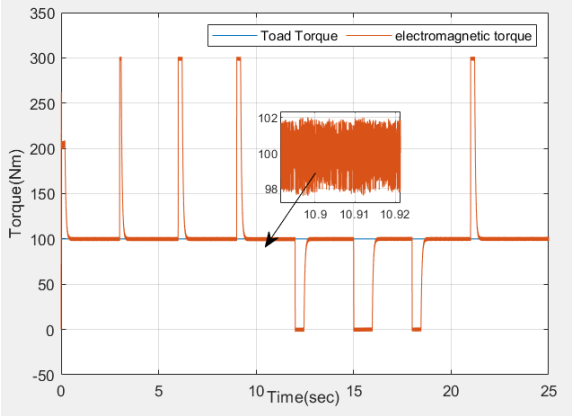

(c) electromagnetic torque result.

Figure 5.4: Performance of MPC controller under variable speed reference.

The above pictures describes the performance of MPC controllers using variable speed range and under constant load torque. So, the actual speed trucks its desired reference with good performance(low steady state error and settling time).

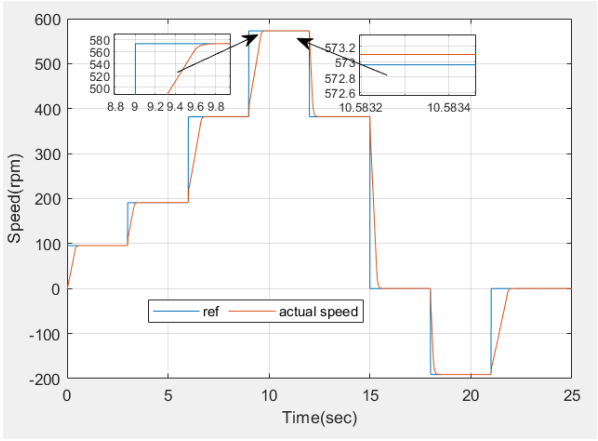

(a) motor speed result.

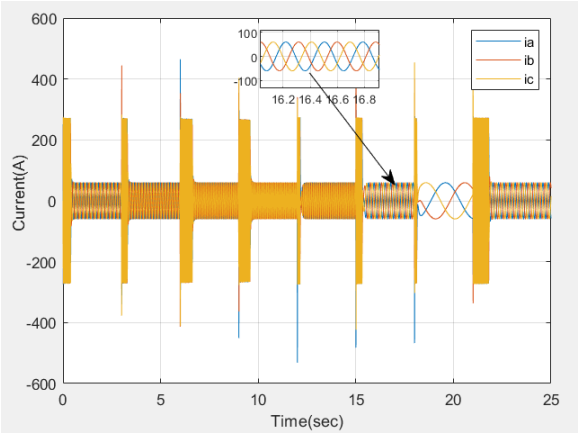

(b) stator current result.

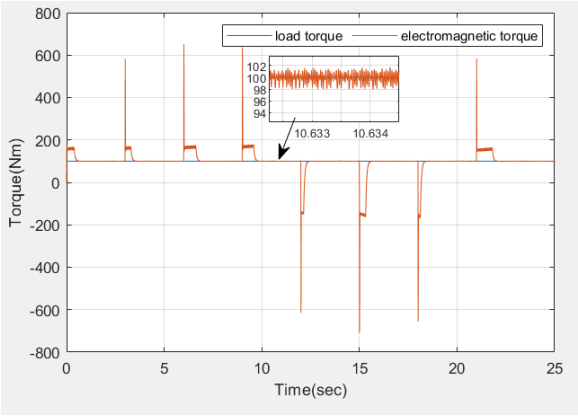

(c) electromagnetic torque result.

Figure 5.5: Performance of ISMC controller under variable speed reference.

Figure 5.5 shows the performance of ISMC controller using variable speed range and as shown in the above picture the speed trucks its desired reference with good performance and the electromagnetic torque have lower ripple.

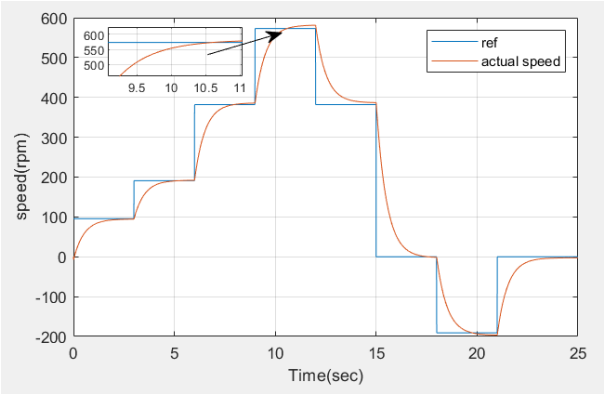

(a) motor speed result.

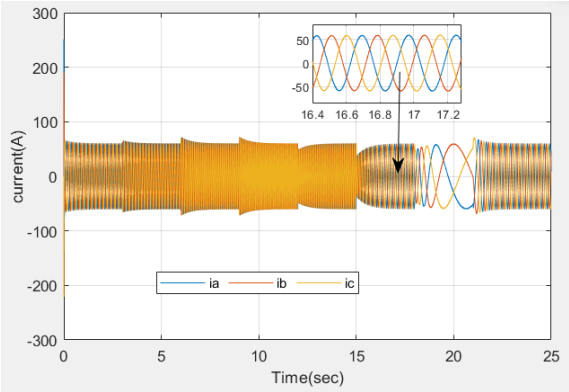

(b) stator current result.

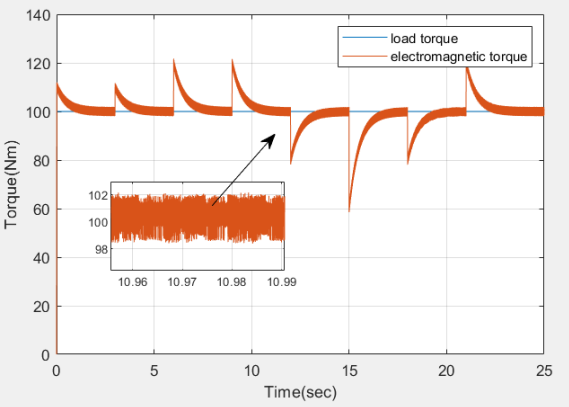

(c) electromagnetic torque result.

Figure 5.6: Performance of LQR controller under variable speed reference.

Figure 5.6 is based on lqr controller and as shown in the above picture it has lower disturbance handling capacity. which means it has high steady-state error and large settling time error over a variable speed range.

5.4 Four Quadrant Operation of IM

The four-quadrant operation of an induction motor refers to its ability to operate in both directions (forward and reverse) and in both the motoring and the generating modes. This capability is crucial for applications requiring precise control, such as in electric vehicles. The figure 5.7 shows a successful operation of IM in four-quadrant to adapt for electric vehicle propulsion.

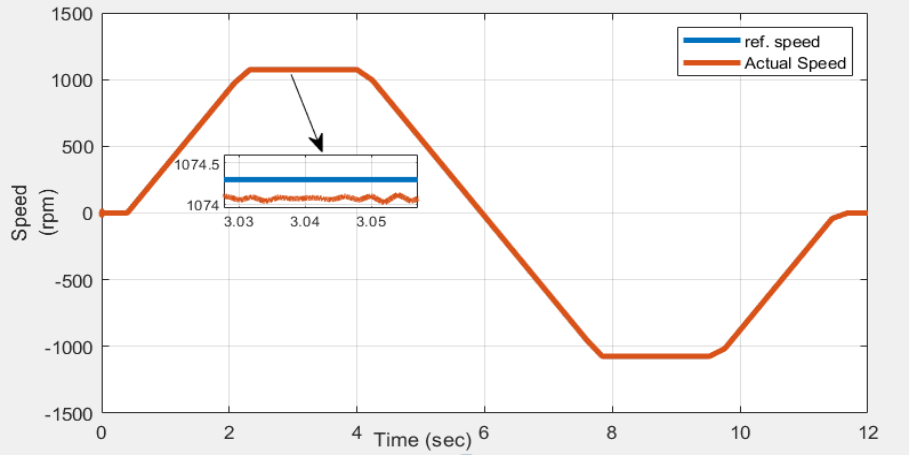

Figure 5.7: Four quadrant operation of IM

Chapter 6

Conclusion and Future Works

6.1 Conclusion

This thesis models the predictive speed and torque control of an induction motor using MATLAB/SIMULINK environment. The motor and controller were modeled using the SIMULINK environment, and the object function for the nonlinear mpc speed controller and the algorithm for the predictive torque controller were developed in a MATLAB environment. Additionally, a two-level voltage source inverter was employed to supply power to the motor.

In this thesis four pole three phase induction motor were used. Their simple design,lower manufacturing costs, robust construction, lack of reliance on rare-earth materials, Wide Operating Speed Range, highly efficient with full-load efficiency ranging from 85% to 97%, easily controlled using advanced control systems, and its scalability making them versatile for various types of EVs.

The simulation result shows how well the suggested speed controller performs. A comparison with the lqr and ISMC speed controller was made in order to demonstrate the efficacy of the suggested controller. The steady state error is -0.0014% for ISMC, 0.025% for lqr, and 0.0004% for mpc, confirming that the mpc has a lower steady-state error than the lqr controller at a constant load torque of 40N.m. The mpc has the ability to reject disturbances, while the lqr has a greater speed drop at the moment of applied load torque. The performance comparison also took into account changing load torque as a disturbance. Overall performance of the model predictive controller is better than the LQR controller.But, it has almost the close result with ISMC controller. Therefore, it is preferable to use MPC and ISMC as the primary controller for IM control in ev applications. To regulate the torque

in response to the speed controller output, a model predictive torque controller is integrated as an inner loop in addition to the speed controller.

Tractive forces for ev application were modeled in MATLAB/SIMULINK and the load curve were plotted and as shown in figure 3.11 tractive force is approximately equal to speed square.

6.2 Future Works

Selecting a weighting factor that is used to maintain the relative balance between stator flux and torque is a key factor in the predictive torque controller model in minimizing torque ripples. In this paper it is expressed as the ratio of rated values of torque and stator flux has good result as shown on the above But, for future work other advanced tuning methods will be considered. In addition, battery design is essential for tractive application, which will be considered in future work.

Bibliography

[1] Tarek Bedida, Salim Makhloufi, Youcef Bekakra, Mostefa Kermadi, Noureddine Bessous, Ridha Kechida, and Djamel Taibi. Predictive torque control of induction motor for rotor bar faults diagnosis. *Energy Reports*, 11:4940–4956, 2024.

[2] Abdelkarim Belbali, Salim Makhloufi, Abdellah Kadri, Laidi Abdallah, and Zemitte Seddik. Mathematical modeling of a three-phase induction motor. In Adel El-Shahat, editor, *Induction Motors*, chapter 7. IntechOpen, Rijeka, 2023.

[3] M El Hachemi Benbouzid. A review of induction motors signature analysis as a medium for faults detection. *IEEE transactions on industrial electronics*, 47(5):984–993, 2000.

[4] Wassim Boudja. Predictive torque and flux control of induction machine. 2017.

[5] Saurabh Chauhan. Motor torque calculations for electric vehicle. *International journal of scientific & technology research*, 4(8):126–127, 2015.

[6] Jun Cui, Matthew Kramer, Lin Zhou, Fei Liu, Alexander Gabay, George Hadjipanayis, Balamurugan Balasubramanian, and David Sellmyer. Current progress and future challenges in rare-earth-free permanent magnets. *Acta Materialia*, 158:118–137, 2018.

[7] Adolfo Dannier, Andrea Del Pizzo, Luigi Pio Di Noia, and Santolo Meo. Integral sliding-mode direct torque control of sensorless induction motor drives. In *2017 IEEE International Symposium on Sensorless Control for Electrical Drives (SLED)*, pages 243–248. IEEE, 2017.

[8] Juan De Santiago, Hans Bernhoff, Boel Ekergård, Sandra Eriksson, Senad Ferhatovic, Rafael Waters, and Mats Leijon. Electrical motor drivelines in

commercial all-electric vehicles: A review. *IEEE Transactions on vehicular technology*, 61(2):475–484, 2011.

[9] Osama S Ebrahim and Praveen K Jain. Lqr-based stator field oriented control for the induction motor drives. In *2008 Twenty-Third Annual IEEE Applied Power Electronics Conference and Exposition*, pages 1126–1131. IEEE, 2018.

[10] N El Ouanjli, A Derouich, A El Ghzizal, S Motahhir, A Chebabhi, Y El Mourabit, and M Taoussi. Modern improvement techniques of direct torque control for induction motor drives-a review. prot control mod power syst 4 (11), 2019.

[11] Adel El-Shahat. Induction motors-recent advances, new perspectives and applications: Recent advances, new perspectives and applications. 2023.

[12] Mahmoud F Elmorshedy, Wei Xu, Fayez FM El-Sousy, Md Rabiul Islam, and Abdelsalam A Ahmed. Recent achievements in model predictive control techniques for industrial motor: A comprehensive state-of-the-art. *IEEE Access*, 9:58170–58191, 2021.

[13] Khalaf Salloum Gaeid, Hew Wooi Ping, and Haider AF Mohamed. Simulink representation of induction motor reference frames. In *2009 International Conference for Technical Postgraduates (TECHPOS)*, pages 1–4. IEEE, 2009.

[14] Cristian Garcia, Jose Rodriguez, Cesar Silva, Christian Rojas, Pericle Zanchetta, and Haitham Abu-Rub. Full predictive cascaded speed and current control of an induction machine. *IEEE Transactions on Energy Conversion*, 31(3):1059–1067, 2016.

[15] Tobias Geyer, Georgios Papafotiou, and Manfred Morari. Model predictive direct torque control—part i: Concept, algorithm, and analysis. *IEEE transactions on industrial electronics*, 56(6):1894–1905, 2008.

[16] Bojan Grčar, Anton Hofer, and Gorazd Štumberger. Induction machine control for a wide range of drive requirements. *Energies*, 13(1):175, 2019.

[17] Joachim Holtz. A predictive controller for the stator current vector of ac machines fed from a switched voltage source. *IPEC-Tokyo, 1983*, pages 1665–1675, 1983.

[18] Swaraj Ravindra Jape and Archana Thosar. Comparison of electric motors for electric vehicle application. *international Journal of Research in Engineering and Technology*, 6(09):12–17, 2017.

[19] V Kousalya and Bhim Singh. Dsvm based predictive torque control of induction motor for ev. In *2020 IEEE International Conference on Computing, Power and Communication Technologies (GUCON)*, pages 284–289. IEEE, 2020.

[20] Paul C Krause, Oleg Wasynczuk, Scott D Sudhoff, and Steven Pekarek. *Analysis of electric machinery and drive systems*, volume 2. Wiley Online Library, 2002.

[21] Rasika R Kulkarni, SP Ghanegaonkar, and VN Pande. Model predictive control (mpc) based voltage control in distribution network with distributed generation. In *2021 4th International Conference on Recent Developments in Control, Automation & Power Engineering (RDCAPE)*, pages 211–216. IEEE, 2021.

[22] Jignesh A Makwana, Pramod Agarwal, and SP Srivastava. Novel simulation approach to analyses the performance of in-wheel srm for an electrical vehicle. In *2011 International Conference on Energy, Automation and Signal*, pages 1–5. IEEE, 2011.

[23] Mohamed Mamdouh and Mohammad Ali Abido. Efficient predictive torque control for induction motor drive. *IEEE Transactions on Industrial Electronics*, 66(9):6757–6767, 2018.

[24] M Github Mehrez. Mpc and mhe implementation in matlab using casadi. *github*, 2022.

[25] A Jan Melkebeek. *Electrical machines and drives: fundamentals and advanced modelling*. Springer, 2018.

[26] Ned Mohan. Electric drives: an integrative approach. *(No Title)*, 2003.

[27] Vishnu Prasad Muddineni, Srinivasa Rao Sandepudi, and Anil Kumar Bonalac. Predictive torque control of induction motor drive with simplified weighting factor selection. In *2016 IEEE international conference on power electronics, drives and energy systems (PEDES)*, pages 1–6. IEEE, 2016.

[28] E Parliament. Co2 emissions from cars: facts and figures (infographics). *European Parliament. https://www. europarl. europa. eu/news/en/headlines/society/20190313STO31218/co2-emissions-from-cars-facts-and-figures-infographics*, 2019.

[29] T Porselvi, MK Srihariharan, J Ashok, and S Ajith Kumar. Selection of power

rating of an electric motor for electric vehicles. *International Journal of Engineering Science and Computing IJESC*, 7(4):6469–6472, 2017.

[30] Punit L Ratnani and AG Thosar. Mathematical modelling of an 3 phase induction motor using matlab/simulink. *International Journal Of Modern Engineering Research (IJMER)*, 4(6):62–67, 2014.

[31] İlker Şahin. *Model predictive torque control of an induction motor enhanced with an inter-turn short circuit fault detection feature*. PhD thesis, Middle East Technical University (Turkey), 2021.

[32] Adeel Saleem, Nain Liu, Hu Junjie, Atif Iqbal, Muhammad Aftab Hayyat, and Muhammad Mateen. Modelling of an electric vehicle for tractive force calculation along with factors affecting the total tractive power and energy demand. In *2020 3rd International Conference on Computing, Mathematics and Engineering Technologies (iCoMET)*, pages 1–5. IEEE, 2020.

[33] IS Selcuk and AM Koktas. Transport sector energy use and carbon emissions: a study on sectoral fiscal policies. *Zeszyty Naukowe Szkoły Głównej Gospodarstwa Wiejskiego w Warszawie. Ekonomika i Organizacja Logistyki*, (5 [3):17–30, 2020.

[34] Seung-Ki Sul. *Control of electric machine drive systems*. John Wiley & Sons, 2011.

[35] Manoj Swargiary, Jayati Dey, and Tapas Kumar Saha. Optimal speed control of induction motor based on linear quadratic regulator theory. In *2015 annual IEEE india conference (indicon)*, pages 1–6. IEEE, 2015.

[36] Bekheira Tabbache, Abdelaziz Kheloui, and MEH Benbouzid. Design and control of the induction motor propulsion of an electric vehicle. In *2010 IEEE Vehicle Power and Propulsion Conference*, pages 1–6. IEEE, 2010.

[37] Junnian Wang, Xu Zhang, and Dan Kang. Parameters design and speed control of a solar race car with in-wheel motor. In *2014 IEEE Transportation Electrification Conference and Expo (ITEC)*, pages 1–6. IEEE, 2014.

[38] Yongchang Zhang, Yubin Peng, and Haitao Yang. Performance improvement of two-vectors-based model predictive control of pwm rectifier. *IEEE Transactions on Power Electronics*, 31(8):6016–6030, 2015.

[39] Yongchang Zhang and Jianguo Zhu. Direct torque control of permanent magnet synchronous motor with reduced torque ripple and commutation fre-

quency. *IEEE Transactions on Power Electronics*, 26(1):235–248, 2010.

[40] Yongchang Zhang, Jianguo Zhu, Zhengming Zhao, Wei Xu, and David G Dorrell. An improved direct torque control for three-level inverter-fed induction motor sensorless drive. *IEEE transactions on power electronics*, 27(3):1502–1513, 2010.

Appendices

Appendix A

MATLAB/SIMULINK Block Diagrams

A.1 Overall SIMULINK Block Diagram

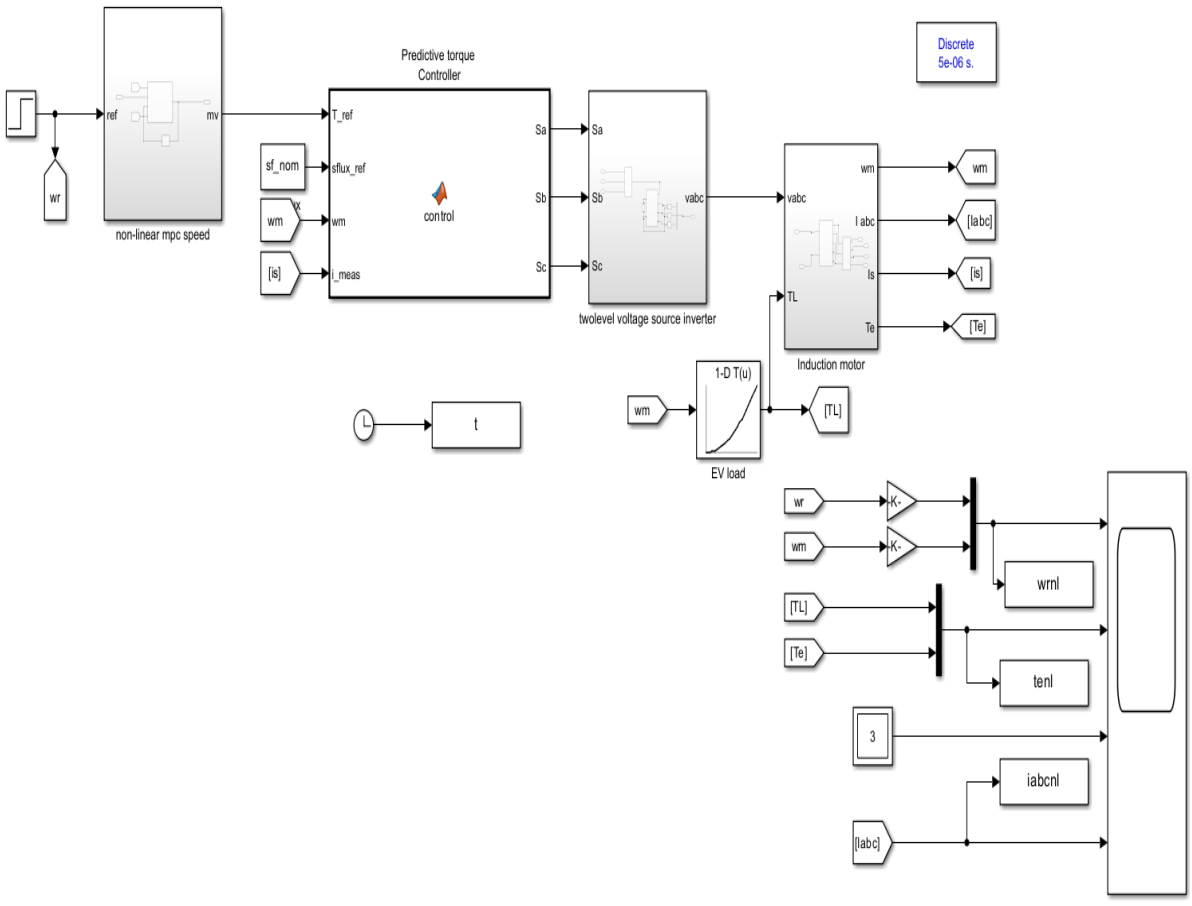

Figure A.1: Over all SIMULINK diagram

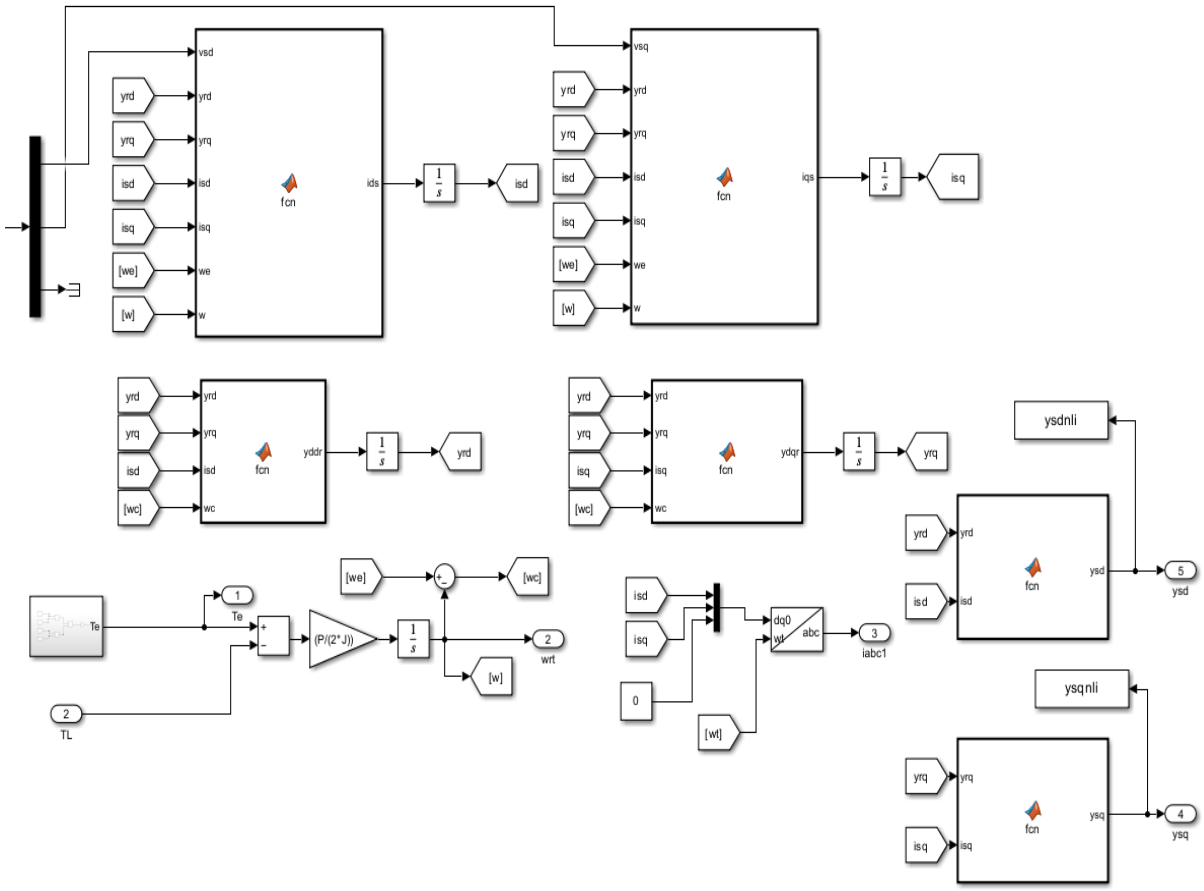

Figure A.2: Induction Motor

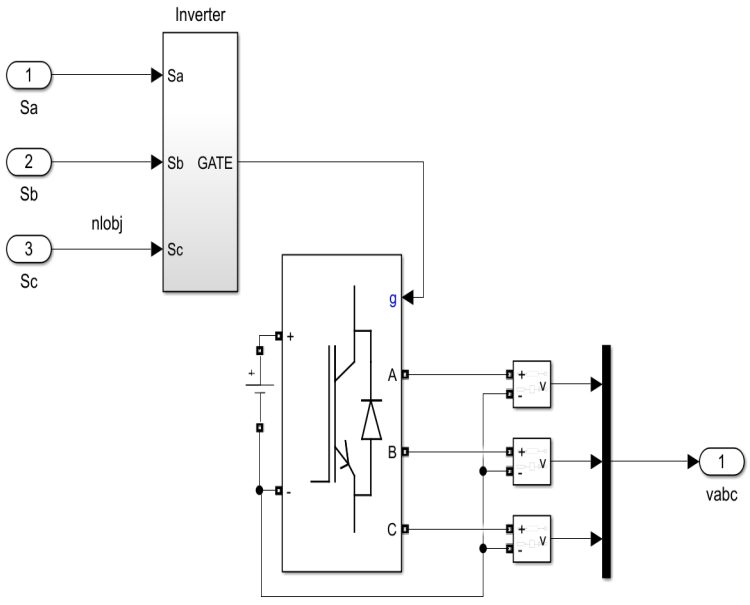

Figure A.3: 2-level voltage source inverter

A.2 SIMULINK Block Diagram Using ISMC

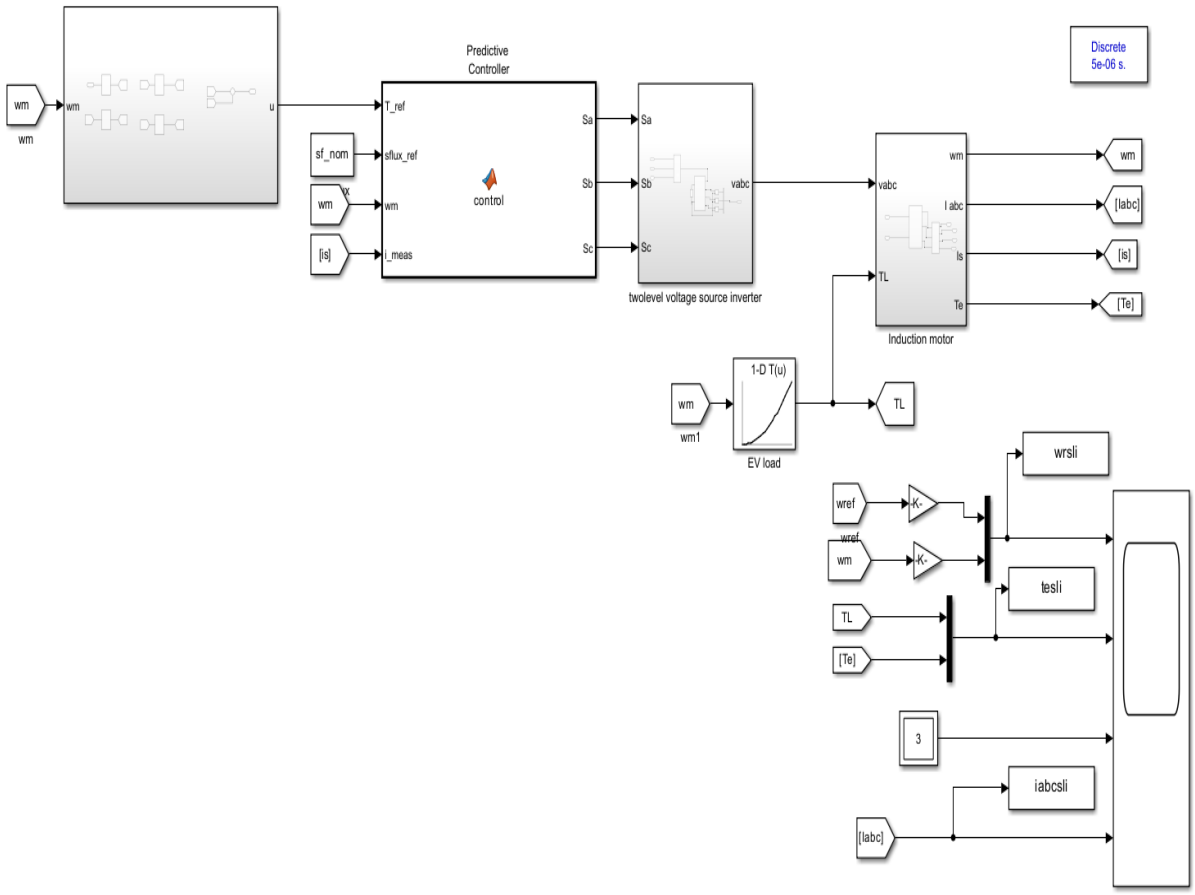

Figure A.4: Over all block diagram using ISMC

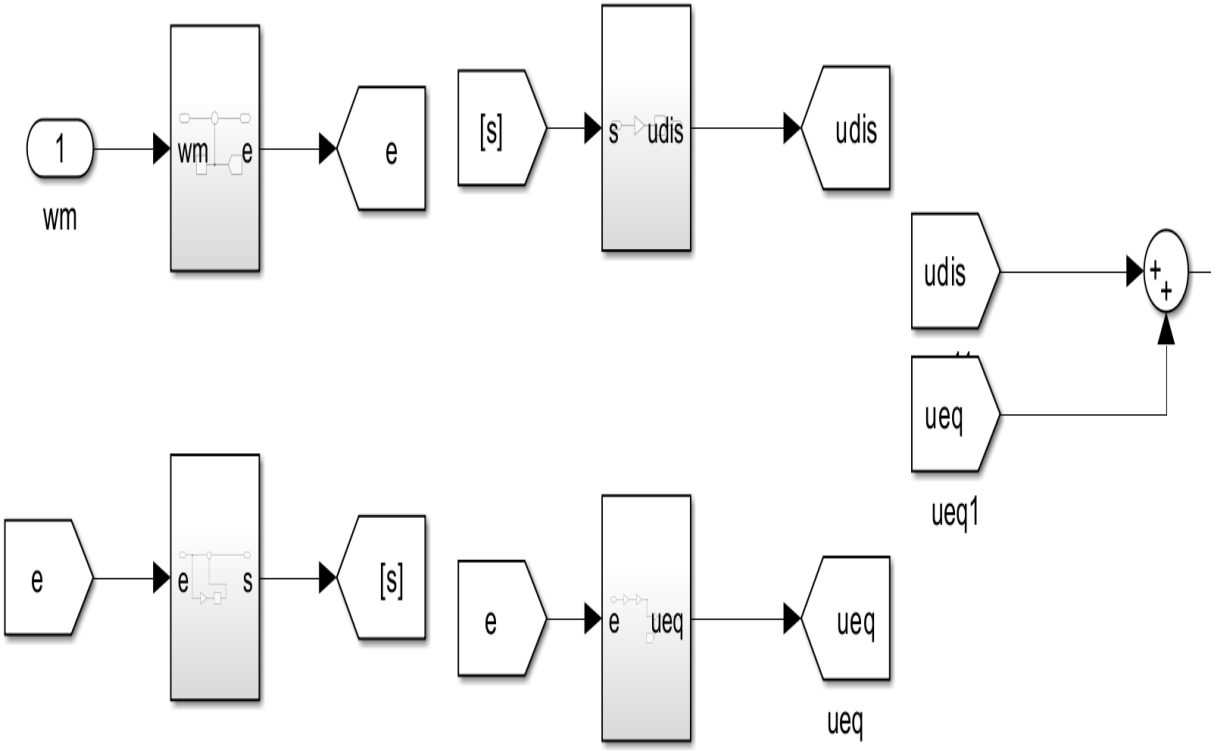

Figure A.5: Integral Sliding Mode Control

Appendix B

MATLAB Codes

B.1 Program for PTC

```
function [Sa,Sb,Sc] = fun(T_ref,sflux_ref,wm,i_meas,Ts,
    Rs,Lr,Lm,Ls,p,tr,kr,r_sigma,t_sigma,lambda,v,states
       )
persistent x_opt Fs
if isempty(x_opt), x_opt = 1; end
if isempty(Fs), Fs = 0 + 0i*1; end
% estimation of stator flux
Fs = Fs + Ts*(v(x_opt) - Rs*i_meas);
% estimation of rotor flux
Fr = Lr/Lm*Fs+i_meas*(Lm-Lr*Ls/Lm);
g = zeros(1,8);
for i = 1:8
    % i-th voltage vector for current prediction
    v_o1 = v(i);
    % Stator flux prediction at instant k+1
    Fsp1 = Fs + Ts*v_o1 - Rs*Ts*i_meas;
    % Stator current prediction at instant k+1
    Isp1 = (1+Ts/t_sigma)*i_meas+Ts/(t_sigma+Ts)*
        (1/r_sigma*((kr/tr-kr*1i*wm)*Fr+v_o1));
    % Torque prediction at instant k+1
    Tp1 = 3/2*p*imag(conj(Fsp1)*Isp1);
    % Cost function
    g(i) =  abs(sflux_ref-abs(Fsp1))+lambda*abs(T_ref -
        Tp1);
```

```
23 end
24 %*************************************
25 % Optimization
26 [~, x_opt] = min(g);
27 % Output switching states
28 Sa = states(x_opt,1);
29 Sb = states(x_opt,2);
30 Sc = states(x_opt,3);
```

B.2 Non-MPC object function

```
mdl = 'nevptcnew';
open_system(mdl)
Ts=0.0002;
nlobj = nlmpc(1,1,'MV',1,'MD',2);
nlobj.Ts = Ts;
nlobj.PredictionHorizon = 20;
nlobj.ControlHorizon = 3;
nlobj.Model.StateFcn = @(x,u) mystatefunction(x,u);
nlobj.Model.OutputFcn = @(x,u) x;
nlobj.MV.Min = 0;
nlobj.MV.Max = 105;

nlobj.MV.ScaleFactor =100;
nlobj.MD.ScaleFactor = 0.5;
nlobj.Weights.OutputVariables = 0.6;
nlobj.Weights.ManipulatedVariablesRate = 0.9;
x0 = 0;
u0 = 0;
ref0 = 104.72;
md0 = out.ev;
validateFcns(nlobj,x0,u0,md0,{},ref0)
```

B.3 MATLAB script file for LQR controller gain k

```
%for lqr controller gain k

f=0.02791;      %Friction cofficient
J = 0.37;         % Moment of inertia [kg m^2]

Lm = 0.0291;       % Magnetizing inductance [H]
Ls = 0.0314;     % Stator inductance [H]
Lr = 0.0291;    % Rotor inductance [H]
Rs = 0.0851;       % Stator resistance [Ohm]
Rr = 0.0658;       % Rotor resistance [Ohm]
%x(t) = Ax(t) + Bu(t)
%dwr(t)/dt = 1/J (  kf  * wr(t) + Te(t)) at zero load
   torque
A=-f/J;
C=1;
D=0;
B=1/J;
%performance index value
Q=0.2443;
R=0.25;
%Design LQR controller assume no tracking
[K_{lqr}, P, E_{ig}]=lqr(A,B,Q,R)
```

B.4 nonlinear mpc controller using casadi at 500rpm and 40Nmload torque

```
clear all
close all
clc
mdl = 'casadi';
open_system(mdl)
addpath('C:\Users\hp\Desktop\casadi\MPC-and-MHE
implementation-in-MATLAB-using-Casadi-master\
 workshop_github\Codes_casadi_v3_5_5\MPC_code ')
 import casadi.*
 % i had one state which is speed x(t) = Ax(t) +Bu(t)+d
 %wr(t) = 1/J (fwr(t) + Te(t)-TL)
 mdl = 'casadi';
 open_system(mdl)
 T = 0.001; % sampling time [s]
 N = 100; % prediction horizon
 J = 0.37;
 % Moment of inertia [kg m^2]
 Lm = 0.0291;
 Ls = 0.0314;
 % Magnetizing inductance [H]
 % Stator inductance [H]
 Lr = 0.0291; % Rotor inductance [H]
 Rs = 0.0851;
 % Stator resistance [Ohm]
 Rr = 0.0658;
 TL=40;
 % Rotor resistance [Ohm]
 Te_max=50; Te_min = 0; %as constraint on
    electromagnetic torque
 x = SX.sym('x'); %define state variable x
 states = x; n_states = length(states);
 Te = SX.sym('Te');
 controls = Te; n_controls = length(controls);
  rhs = ((2/J)*(Te-TL)); % system r.h.s
  f = Function('f',{states,controls},{rhs}); %
     nonlinear  mapping function f(x,u)
```

```
35
36  U = SX.sym('U',n_controls,N); % Decision variables (
       controls)
37  P = SX.sym('P',n_states + n_states);% parameters (
       which include the initial and the reference state
       of the equation)
38 X = SX.sym('X',n_states,(N+1));% A Matrix that
     represents the states over the optimization problem
     .
39 obj = 0; % Objective function
40 g = []; % constraints vector
41 Q =0.25; % weighing matrices (states)
42 R =0.25; % weighing matrices (controls)
43 st = X(:,1); % initial state
44 g = [g;st-P(1)]; % initial condition constraints
45 for k = 1:N
46 st = X(:,k); con = U(:,k);
47 end
48 obj = obj+(st-P(2))'*Q*(st-P(2)) + con'*R*con; %
     calculate obj
49 st_next = X(:,k+1);
50 f_value = f(st,con);
51 st_next_euler = st+ (T*f_value);
52 g = [g;st_next-st_next_euler]; % compute constraints
53 % make the decision variable one column vector
54 OPT_variables = [reshape(X,1*(N+1),1);reshape(U,1*N,1)
55 ];close
56 nlp_prob = struct('f', obj, 'x', OPT_variables, 'g', g
     ,
57 'p', P);
58 opts = struct;
59 opts.ipopt.max_iter = 8000;
60 opts.ipopt.print_level =1;%0,3
61 opts.print_time =1;
62 opts.ipopt.acceptable_tol =1e-8;
63 opts.ipopt.acceptable_obj_change_tol = 1e-6;
64 solver = nlpsol('solver', 'ipopt', nlp_prob,opts);
65 args = struct;
66 args.lbg(1:1*(N+1)) = 0; % Equality constraints
```

```
67  args.ubg(1:1*(N+1)) = 0; % Equality constraints
68  args.lbx(1:1:1*(N+1),1) = 0; %state x lower bound
69  args.ubx(1:1:1*(N+1),1) =157.08; %state x upper bound
70  args.lbx(1*(N+1)+1:1:1*(N+1)+1*N,1) = Te_min; %v lower
        bound
71  63 args.ubx(1*(N+1)+1:1:1*(N+1)+1*N,1) = Te_max; %v
       upper bound
72  %---------------------------------------------
73 %-----------------------------------------
74  t0 = 0;
75  x0 = 0; % initial condition.
76  xs =52.36; % Reference posture.
77  xx(:,1) = x0; % xx contains the history of states
78  t(1) = t0;
79  u0 = zeros(N,1);
80  % control input to the motor
81  X0 = repmat(x0,1,N+1)'; % initialization of the states
        decision variables
82  sim_tim =5; % Maximum simulation time
83  mpciter = 0;% Start MPC
84  xx1 = [];
85  u_cl=[];
86   % the main simulaton loop... it works as long as the
        error is greater
87   % than 10^-6 and the number of mpc steps is less than
         its maximum
88   % value.
89   tic
90   while(norm((x0-xs),2) > 1e-2 && mpciter < sim_tim / T
        )
91  args.p = [x0;xs]; % set the values of the parameters
       vector
92  % initial value of the optimization variables
93  args.x0 = [reshape(X0',1*(N+1),1);reshape(u0',1*N
94  ,1)];
95  sol = solver('x0', args.x0, 'lbx', args.lbx, 'ubx',
96  args.ubx,...
97  'lbg', args.lbg, 'ubg', args.ubg,'p',args.p);
```

```
u = reshape(full(sol.x(1*(N+1)+1:end))',1,N)'; % get
   controls only from the solution
xx1(:,1:1,mpciter+1)= reshape(full(sol.x(1:1*(N+1))
)',1,N+1)'; % get solution TRAJECTORY
u_cl= [u_cl ; u(1,:)];
t(mpciter+1)= t0;
 %Applythecontrolandshiftthesolution
 [t0,x0,u0]= shift(T,t0,x0,u,f);
 xx(:,mpciter+2)=x0;
 X0=reshape(full(sol.x(1:1*(N+1)))',1,N+1)'; %get
    solutionTRAJECTORY
%Shifttrajectorytoinitializethenextstep
X0=[X0(2:end,:);X0(end,:)];
mpciter
mpciter=mpciter+1;
 end;
 toc
 ss_error=norm((x0-xs),2)
 teref=u(1)
```